Phenotyping of *Cercospora beticola* resistance of sugar beet genotypes by hyperspectral imaging

Dissertation

zur Erlangung des Grades

Doktorin der Agrarwissenschaften (Dr. agr.)

der Landwirtschaftlichen Fakultät
der Rheinischen Friedrich-Wilhelms-Universität Bonn

von

Marlene Leucker

aus
Marburg

Bonn 2018

Referent: PD Dr. Erich-Christian Oerke

Korreferent: Professor Dr. Jens Léon

Tag der mündlichen Prüfung: 27.04.2018

Angefertigt mit Genehmigung der Landwirtschaftlichen Fakultät der Universität Bonn

Jedes Naturgesetz, das sich dem Beobachter offenbart,

lässt auf ein höheres, noch unerkanntes schließen.

Alexander von Humboldt (1845) *Kosmos* Band 1:21

ABSTRACT

Cultivation of disease resistant crops is an important strategy in the integrated pest management which is a guiding principle for good agricultural practice. Therefore, high yielding cultivars with resistance to important plant diseases are needed. The integration of resistance sources such as wild relatives or compatible subspecies might help to enhance the resistance of crops and thus to reduce the need for chemical crop protection measures. For the selection of plants with a specific trait, such as resistance to a plant pathogen, precise determination of the genotype and a reliable characterization of the phenotype are necessary. The rather rapid development of molecular methods and knowledge about genes enhanced the genotyping in plant breeding greatly. The phenotyping, however, is still the bottleneck in resistance breeding. As the phenotype is the result of the interaction of the genotype and the environment phenotyping must be reliable, reproducible and non-invasive. The implementation of sensors in phenotyping systems provides many advantages. Hyperspectral imaging sensors are well suited to characterize different plant traits. Cercospora leaf spot (CLS) is the most important foliar disease of sugar beets and is mainly controlled by fungicide applications. The aim of this study was to characterize the resistance of sugar beet genotypes against *Cercospora beticola* and the development of a hyperspectral imaging system for phenotyping this disease resistance.

A hyperspectral microscope that measures reflection in the visible and near-infrared range from 400 to 1000 nm with a magnification of up to 7.3x was established to determine spectral changes on the plant tissue level. Disease development on five genotypes infected with CLS was evaluated and compared under controlled conditions. Two additional genotypes were used to validate the results of the hyperspectral measurement of CLS dynamics.

Resistant genotypes had a lower percentage of diseased leaf area, a reduced number of lesions, lesion size and growth rate and a decreased spore production. Apart from the quantitative difference between highly susceptible and more resistant sugar beets, the lesion phenotype varied in size and spatial composition depending on the host genotype. Using the hyperspectral microscope, lesions could be differentiated into subareas based on their spectral characteristics. Sugar beet genotypes with lower disease severity typically had lesions with smaller centers and produced fewer spores in comparison to highly susceptible genotypes. The differences in number of spores per lesion were closely associated to the spectral difference calculated as area between spectral signatures before and after sporulation. The CLS development, analyzed by hyperspectral imaging over ten days, differed depending on the host genotype and the resistance source. For example, lesion development on a resistant genotype carrying two quantitative trait loci (QTL) was characterized by a fast and abrupt change in spectral reflectance, whereas it was slower and ultimately more severe on the closely related genotype lacking the QTL. The analysis of reflectance and transmittance images by calculating spectral vegetation indices and extracting spectral signatures revealed a potential benefit of transmission measurements. Depending on the topic and analysis method, effects were sometimes stronger pronounced in the transmittance data.

The resistance against C. *beticola* was not complete, instead, it can be described as quantitative and rate-reducing. Some resistance parameters such as a decreased sporulation matter particularly with regards to disease epidemics in the field. Based on the hyperspectral images, a detailed analysis of the lesions was possible. The presented method allowed a reliable differentiation of CLS dynamics and the characterization of even subtle differences in resistance. Hyperspectral imaging is a promising tool with the potential to improve the screening process in breeding for CLS resistance.

ZUSAMMENFASSUNG

Der Anbau von krankheitsresistenten Nutzpflanzen ist eine wichtige Strategie im integrierten Pflanzenschutz, der ein zentraler Bestandteil der guten fachlichen Praxis in der Landwirtschaft ist. Daher sind Hochleistungssorten mit Resistenzen gegen bedeutende Pflanzenkrankheiten erforderlich. Die Integration von Resistenzquellen, wie zum Beispiel verwandte Wildarten, oder kompatible Subspezies können dazu beitragen, die Resistenz der Pflanzen zu verbessern und so den Einsatz chemischer Pflanzenschutzmittel zu verringern. Für die Selektion von Pflanzen mit einem Merkmal, wie der Resistenz gegen ein Pathogen, sind eine präzise Bestimmung des Genotyps und eine zuverlässige Charakterisierung des Phänotyps notwendig. Die Genomanalyse und Identifizierung beteiligter Gene ist dank moderner molekularer Methoden weit fortgeschritten, doch stellt die Phänotypisierung noch einen Engpass in der Pflanzenzüchtung dar. Da die Merkmalsausprägung einer Pflanze das physikalische Ergebnis der Wechselwirkung zwischen dem Genotyp und der Umwelt ist, muss die Phänotypisierung zuverlässig, reproduzierbar und möglichst nicht-invasiv sein. Der Einsatz von optischen Sensoren bietet daher viele Vorteile bei der Phänotypisierung. Abbildende Hyperspektralsensoren eignen sich gut, um verschiedene Pflanzeneigenschaften zu charakterisieren.

Cercospora-Blattflecken (CBF) sind die wichtigste Blattkrankheit der Zuckerrübe und wird hauptsächlich durch den Einsatz von Fungiziden kontrolliert. Ziel dieser Arbeit war die Charakterisierung der Resistenz von Zuckerrüben-Genotypen gegenüber *Cercospora beticola* und die Entwicklung eines hyperspektralen Sensorsystems für die Phänotypisierung dieser Krankheitsresistenz.

Ein hyperspektrales Mikroskop, das die Reflektion im sichtbaren und nahen-infrarotem Bereich von 400 bis 1000 nm misst, wurde entwickelt. Die bis zu 7.3fache Vergrößerung ermöglichte die Erfassung spektraler Änderungen auf Gewebeebne. An fünf mit CBF infizierten Genotypen wurde der Krankheitsverlauf unter Gewächshausbedingungen untersucht und verglichen. Zwei weitere Genotypen wurden verwendet um die Ergebnisse der hyperspektralen Messungen der CBF-Entwicklung zu validieren.

Resistente Genotypen wiesen einen geringeren Anteil befallener Blattfläche, eine reduzierte Anzahl, Größe und Wachstumsrate der Läsionen sowie eine verringerte Sporulation auf. Abgesehen von den quantitativen Unterschieden zwischen hochanfälligen und resistenten Zuckerrüben, variierte der Läsionsphänotyp in der Größe und räumlichen Zusammensetzung in Abhängigkeit des Wirtsgenotyps. Mit Hilfe des hyperspektralen Mikroskops konnten Läsionsbereiche anhand ihrer spektralen Eigenschaften differenziert werden. Resistentere Genotypen hatten typischerweise Läsionen mit kleineren Zentren und geringerer Sporulation verglichen mit anfälligen Genotypen. Die Unterschiede in der Anzahl der gebildeten Sporen waren eng mit der spektralen Differenz, die als Fläche zwischen den spektralen Signaturen vor und nach Sporenbildung berechnet wurde, verbunden. Die CBF-Entwicklung, analysiert über zehn Tage anhand der spektralen Signaturen, unterschied sich in Abhängigkeit von dem Wirtsgenotyp und der Resistenzquelle. Zum Beispiel war die Ausbildung der Läsionen auf einem Genotyp mit zwei Quantitative Trait Loci (QTL) durch eine schnelle und abrupte Veränderung der spektralen Reflektion charakterisiert, dahingegen war die Entwicklung auf einem nah verwandten Genotyp ohne QTL langsamer, aber letztlich stärker. Die Analyse von Reflexions- und Transmissionsaufnahmen anhand der Berechnung von spektralen Vegetationsindizes und der Extraktion spektraler Signaturen zeigte einen möglichen Nutzen der Transmissionsmessungen. In Abhängigkeit von der Fragestellung und Analysemethode waren die Effekte in der Transmission manchmal stärker ausgeprägt.

Die Resistenz der Genotypen gegen *C. beticola* war quantitativ und der CBF-Befall wurde nicht vollständig verhindert; stattdessen breitete sich der Befall langsamer und weniger stark aus. Charakteristisch war auch eine verringerte Sporenbildung, die im Hinblick auf die Verbreitung der Krankheit im Feld eine entscheidende Rolle spielt. Anhand der hyperspektralen Bilder war eine detaillierte Analyse der Symptome und deren Entwicklung sowie die Charakterisierung feiner Unterschiede in der CBF-Resistenz möglich. Hyperspektrale Messungen sind ein vielversprechendes Werkzeug mit dem Potenzial zur Verbesserung des Selektions-Verfahrens in der Resistenzzüchtung.

Contents

1 INTRODUCTION

Integrated pest management (IPM) is a guiding principle for the good agricultural practice and is anchored in the German Plant Protection Act and the Directive of the European Union from 2009 (Directive 2009/128/EG). It is a system which uses all economically, environmentally and toxicologically appropriate methods to keep plant pests and diseases under the economic threshold level. The best combination of biological, biotechnical, agricultural, plant production and breeding measures is supposed to limit the chemical crop protection to the minimum amount necessary (Wetzel *et al*. 2008). The cultivation of disease resistant crops is an important strategy in IPM. Disease resistance inhibits or reduces the disease outbreak or spreading; thus, reducing the need for chemical crop protection measures. Therefore, there is a high demand for varieties which combine effective resistance and high productivity. The integration of resistance genes, for example, from wild relatives or mutant populations might help to enhance the given resistance of crops. In grapevine, for example, the resistance locus *Rpv3,* originated from a wild vine (*Vitis rupestris*), was introgressed in many varieties and confers a high degree of resistance to downy mildew (Fischer *et al*. 2004; Di Gaspero *et al*. 2012).

For a successful selection of plants with a specific trait, such as resistance to a specific plant pathogen, the identification of the genetic basis for this trait and the linkage to the phenotype are necessary. The rather rapid development of molecular methods and genome analysis as well as the growing knowledge about genomes and involved genes enhanced the genotyping in plant breeding greatly. Marker-assisted selection methods are used to track and accumulate desired gene loci. Also, more and more genomes of important crops are sequenced (Feuillet *et al*. 2011). As the phenotype is the physical result of the interaction of the genotype and the diverse environment, repeated trials in multiple environments are necessary over several years (Furbank and Tester 2011). Due to the (necessity for) time-consuming and cost-intensive efforts, phenotyping is still the bottleneck in resistance breeding.

Over the years, optical sensor technologies have been investigated as potential tools for non-destructive and precise analysis of plant phenotypes. Especially, imaging systems are widely established in observing plants responding to (biotic or abiotic) stresses (Mahlein 2016). These technologies provide spatial information obtained in monochromatic or color images and allow a pixel-wise analysis. Various studies were conducted analyzing plant diseases from canopy to cell level (West *et al*. 2003; Mahlein 2016). Common imaging systems are used for color, shape, size or surface texture and they are applied to estimate, for example, the diseased leaf area or the identification of diseases (Barbedo *et al*. 2016). Another well-developed technology to investigate plant characteristics is spectroscopy. It is often based on point measurements which average the reflection, transmission, or absorption of light over a given field of view. The non-spatial spectral information can also be used for the evaluation of chemical properties of objects like water status, nitrogen content or leaf pigment content (Gitelson *et al*. 2009). Hyperspectral imaging (HSI) combines the features of imaging systems and spectroscopy; hence HSI can simultaneously acquire both spatial and spectral information. Electromagnetic spectra (spectral signatures) from visible to infrared wavelengths are acquired for every pixel of an image resulting in a three-dimensional data cube. The spectral information may contain reflection or transmission values depending on the measurement setup.

The optical properties of plants are influenced by the morphology and the biochemical composition of the plant tissue (Govaerts *et al*. 1996). The strong absorption in the visible range (VIS, 400 to 700 nm) is mainly caused by pigments and is typical for optical leaf characteristics (Jacquemoud and Ustin 2001; Jensen 2007). An increased reflection in the near-infrared range

(NIR, 700 to 1100 nm) results from multiple scattering processes, depending on the leaf surface and the internal cell structure. Plant compounds and water influence the light absorption in the shortwave infrared (SWIR, 1100 to 2500 nm) (Jacquemoud and Ustin 2001). The interaction between the plant and a pathogen leads to structural and metabolic modifications which change the spectral characteristics. These effects on leaf reflection and transmission provide the basis for spectral investigations on disease phenotypes. Most research in this field was done measuring hyperspectral reflectance, probably because the measurement procedure is not as complex as for transmission and can also be performed remotely; for example, apples were analyzed for apple scab, cereals for fungal infections, maize for insects and grapevine for downy mildew (Delalieux *et al*. 2007; Carroll *et al*. 2008; Kuska *et al*. 2015; Wahabzada *et al*. 2015; Oerke *et al*. 2016). The host-pathogen interaction of sugar beet (*Beta vulgaris*) and *Cercospora beticola* served as model system in several HSI studies (Rumpf *et al*. 2010; Mahlen *et al*. 2012; 2013; Bergsträsser *et al*. 2015; Arens *et al*. 2016).

Cercospora leaf spot (CLS) is the most important foliar disease of sugar beets (Holtschulte *et al*. 2000). The fungus can produce up to six generations within a growing season and a severe disease outbreak in sugar beet fields may cause yield losses up to 43% (Shane and Teng 1992). CLS is mainly controlled by several fungicide applications. The breeding of sugar beets resistant to *C. beticola* becomes even more important, because there is an increasing occurrence of isolates resistant to strobilurin and benzimidazole fungicides (Karaoglanidis *et al*. 2000; Kirk *et al*. 2012; Trkulja *et al*. 2012). Infected leaves exhibit reddish-brown lesions with a white to grayish center in which black pseudostromata are formed. In later stages, lesions coalesce and may cause complete collapse of the leaves. Detailed microscopic studies have been conducted to reveal processes during pathogenesis. *C. beticola* enters the host through stomata and colonizes the leaf tissue intercellularly (Steinkamp *et al*. 1979; Feindt *et al*. 1981). The pathogen produces toxins such as cercosporin and beticolins in order to necrotize plant cells and make nutrients available (Daub and Ehrenshaft 2000; Goudet *et al*. 2000). This leads to an almost simultaneous collapse of the cells in the infected area. The hyphae grow densely and form pseudostromata below stomata. Melanized conidiophores emerge in the necrotic center of the lesion and produce long, acicular conidia which may be spread by wind or water droplets to infect new leaves or plants (Weiland and Koch 2004). Except one reported example of race-specific, monogenic resistance, CLS resistance is described as quantitative and rate limiting (Lewellen and Whitney 1976; Rossi *et al*. 1999).

The aim of this study was to characterize the quantitative *C. beticola* resistance of different sugar beet genotypes and to develop an HSI system for phenotyping differences in resistance. Therefore, CLS lesions on sugar beet genotypes with varying disease susceptibility were analyzed by classical quantitative methods and a hyperspectral microscope which measures the reflection on the leaf tissue level. Furthermore, simultaneously recorded reflection and transmission images on the leaf level were analyzed to examine the benefit of transmission measurements in addition to the common reflection measurements.

2 MATERIALS AND METHODS

2.1 Plant material

Homozygous sugar beet (*Beta vulgaris* L. spp. *vulgaris*) inbreed lines (Table 1; KWS SAAT SE, Einbeck, Germany) with different susceptibility to *Cercospora beticola* Sacc. were chosen for the experiments. Differences in susceptibility have been assessed in multi-year field trials from the sugar beet breeding program by the breeder KWS SAAT SE. Genotype Bv1+Q and Bv2-Q have been bred from the same resistance source. While Bv1+Q carries the alleles of the resistant parent in two quantitative trait loci (QTL), Bv2-Q does not. The third genotype Bv4_r was developed from another different resistant source. The sugar beet lines Bv6_s and Bv7_s were highly susceptible genotypes. To validate the results of the hyperspectral measurements Bv8 and Bv9 with the same resistance source as Bv1+Q and Bv4, respectively were used.

Sugar beet seeds were pre-grown in small pots until growth stage 12 (GS, Meier 2001). Seedlings were transferred into commercial substrate (Einheitserde ED73, Klasmann-Deilmann, Geeste, Germany) in single plastic pots (Ø 13 cm). Plants were cultivated under controlled conditions at 22°C day and 20°C night temperature, $60 \pm 10\%$ relative humidity (RH) and a photoperiod of 16 h. Plants were watered as necessary and protected against powdery mildew by regular application of sublimate sulfur. Six weeks after transplanting, the sugar beets were fertilized weekly with a 0.2% solution of Poly Crescal (Aglukon GmbH, Düsseldorf, Germany). Plants with six fully developed leaves (GS 16) were used for the experiments after washing off the sulfur.

Table 1: Sugar beet genotypes used in this study and details on designation

Genotype	Resistance source based on information from KWS	Designation in	
		Leucker *et al*. 2016	Leucker *et al*. 2017
Bv1+Q	A	Bv1	Bv1+2+
Bv2-Q	A	Bv2	Bv1-2-
Bv4_r	B	Bv4	-
Bv6_s	-	Bv6	-
Bv7_s	-	Bv7	-
Bv8	A	-	-
Bv9	B	-	-

2.2 Pathogen and inoculation

Inoculum of *C. beticola* for greenhouse experiments was harvested from heavily diseased sugar beet leaves that had been sampled from field crops in late summer. The dry leaves were wetted and incubated at 100% RH for 48 h. Conidia were washed off with a 0.01% solution of polysorbate 20 (Tween® 20, Merck Millipore, Darmstadt, Germany) and a spore suspension with 4×10^4 conidia mL^{-1} was sprayed onto sugar beet leaves. After inoculation, plants were incubated at 100% RH and 25°C day and 20°C night temperature for 48 h. Then, sugar beets were placed back to 60% RH.

2.3 Disease assessment

Disease severity was assessed by visual rating of the percentage diseased leaf area of two fully developed leaf pairs. In addition, the number of lesions per leaf was counted every second day

throughout the experiments. Lesions were examined using a stereo microscope (MZ16 F, Leica Microsystems, Wetzlar, Germany) and images were taken with a mounted digital camera (KY-F75U, JVC, Yokohama, Japan). To investigate the growth rate of CLS, the size of at least 10 developing lesions was measured every day. The size of approximately 100 mature lesions on each genotype was measured to assess different lesion phenotypes on sugar beets. When visible, lesion centers were also measured, and the size of the darker margin was calculated as difference between total lesion area and central area. The different lesion phenotypes were categorized based on the calculated center to margin ratio.

2.4 Measurement of spore production

Spore production was measured on infected sugar beet genotypes according to Karadimos *et al.* (2005). Sporulation was induced by incubating diseased plants at 100% RH for 48 h in the greenhouse. Leaf disks (Ø 11 mm) with a single lesion each were separately placed into 0.5 ml tap water with 0.01% polysorbate 20 (Merck Millipore) and vigorously shaken for 30 s to detach spores from conidiophores. Then, spores were counted using a Fuchs-Rosenthal chamber and the corresponding lesion size was measured using a stereo microscope as described above. Twenty lesions per genotype were analyzed and results expressed as the number of conidia per square millimeter diseased leaf area.

2.5 Hyperspectral measurements and data processing

A hyperspectral microscope was developed to measure spectral reflectance one the leaf tissue level. A spectral line scanner (Spectral camera PFD V10E, Spectral Imaging Ltd., Oulu, Finland) was mounted on a Leica Z6 APO zoom system (Leica Microsystems) with a magnification of up to 7.3x. A 150 W halogen tungsten lamp connected to two linear light emitters (Schott AG, Mainz, Germany) with a vertical orientation of 30° and a distance of 20 cm to the sample was used for homogenous illumination. For image recording the leaf samples were moved with an XY-motorized stage (Prior Scientific GmbH, Jena, Germany). The software SpectralCube (Spectral Imaging Ltd.) was used for controlling the HSI line scanner and for recording the hyperspectral images. To take images of the leaf tissue, samples were 4-fold magnified and a spectral binning of 4 and spatial binning of 1 were chosen. The scan speed was attuned to the chosen magnification and the frame rate was set to 10 frames per second (fps). The exposure time was adjusted to each object to avoid oversaturation.

Simultaneous recording of reflection and transmission of sugar beet leaves were performed using two hyperspectral line scanners (ImSpector V10E, Spectral Imaging Ltd.), with a spectral range from 400 to 1000 nm (Figure 1). Both cameras were oppositely mounted on an aluminium frame with a distance of 60 cm. Plant samples were placed on the motorized stage and the fixed leaves could be moved along the camera's field of view. Four ASD- Pro-Lamps (Analytic Spectral Devices (ASD), Boulder, USA) with a vertical orientation of 36° and a distance of 30 cm to the targets were used for constant illumination from above. The transmission camera was protected from directly incoming light by a black cover. Both camera systems were focused manually to a calibration bar (Spectral Imaging Ltd), positioned in the same distance to the camera as the samples. Images of leaves were taken with spectral binning 4 and spatial binning 1. The frame rate was set to 10 fps and the exposure time was adjusted to the target.

The reflectance or transmittance of samples was calculated by normalizing the images relative to the reflectance of a 100% white reference standard (Zenith Polymer Target, SphereOptics GmbH, Uhldingen-Mühlhofen, Germany) and to a dark current measurement using

4

the ENVI 5.1 + IDL 8.3 software (ITT Visual Information Solutions, Boulder, USA). A 50% diffuser transmission sheet (SphereOptics GmbH) was used instead to calculate transmittance. Before analysis, spectral signals were smoothed by applying the Savitzky-Golay filter (Savitzky and Golay, 1964).
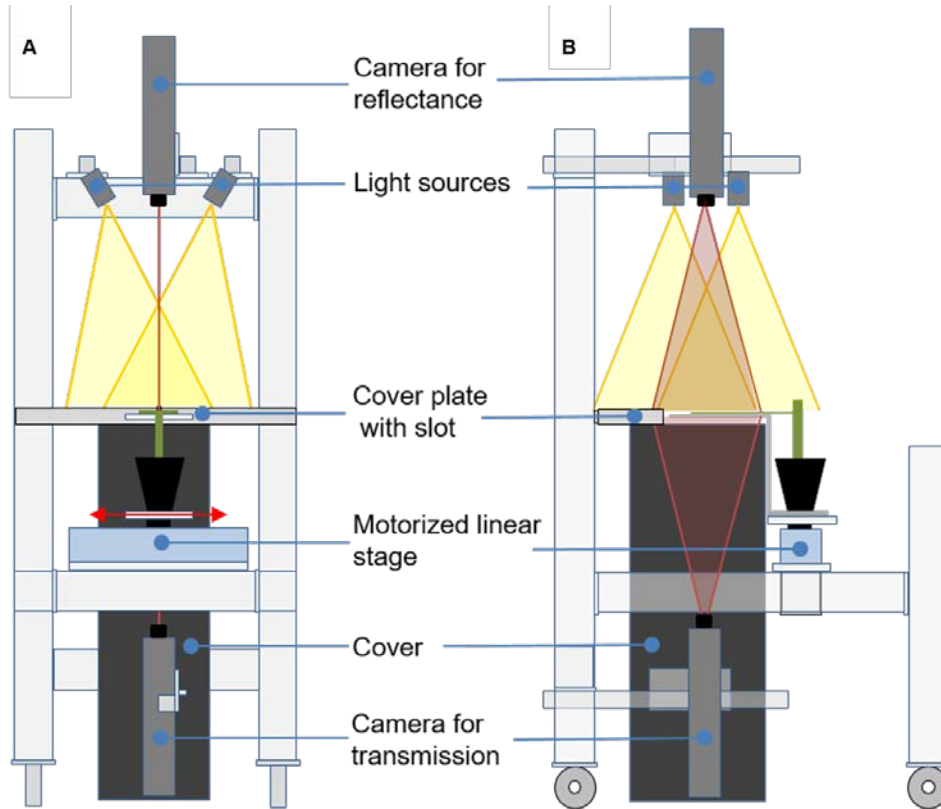

Figure 1: Measurement setup in (A) front and (B) side view for simultaneous recording of reflection and transmission of leaves with two hyperspectral line scanners. The transmission camera is protected from directly incoming light by a black cover. Plant samples are placed on the motorized linear stage and can be moved along the camera's field of view.

2.6 Image analysis

Spectral signatures were manually extracted from pre-processed images as average reflectance of regions of interest (ROI), like non-infected (healthy) tissue as well as a whole lesion, lesion margin or center using ENVI 5.1. To compare spectra of reflectance and transmittance images, difference spectra were calculated by subtracting spectral signatures of non-infected tissue from signatures of lesion center or margin. According to the assumption that the sum of reflectance and transmittance and absorption equals to 1, absorption was calculated as 1 – (reflectance + transmittance). Absorption was computed along a transect through a CLS lesion.

To evaluate spectral differences induced by the sporulation of *C. beticola* the areas between spectral signatures of lesions before (19 dai) and after sporulation (21 dai) were calculated for each genotype. Hyperspectral reflectance of sporulating tissue was also measured before and after

removal of conidia. Additionally, spores protruding out of the lesion were measured laterally to minimize the proportion of the reflectance of the infected tissue below the conidia.

The supervised classification of the hyperspectral images allows a categorization of single image pixels. The image elements are assigned to one out of four predefined classes based on the similarity to the distinct reference spectra (endmembers) of the respective class. The Spectral Angle Mapping method (SAM, Yuhas *et al*. 1992) was performed using the ENVI 5.1 + IDL 8.3 software. For CLS classification the categories 'center', 'transition area', 'margin' and 'non-infected' were defined. The classification converted the hyperspectral image into a pseudo-color image. Non-classified pixels were represented in black.

Spectral vegetation indices (SVI) were calculated using single wavelengths (R, Table 2) and were determined for the same ROI. Single data points for the Anthocyanin reflectance index (ARI) and Photochemical reflectance index (PRI) were obtained along a transect through a CLS lesion to compare reflectance and transmittance data.

Table 2: Spectral vegetation indices used in this study

Spectral vegetation index (SVI)	Equation	Reference
Anthocyanin reflectance index (ARI)	$(1/R_{550})-(1/R_{700})$	Gitelson *et al*. 2001
Cercospora leaf spot index (CLSI)	$(R_{698}-R_{570})/(R_{698}+R_{570})-R_{734}$	Mahlein *et al*. 2013
Photochemical reflectance index (PRI)	$(R_{531}-R_{570})/(R_{531}+R_{570})$	Gamon *et al*. 1992
Pigment specific simple ratio (PSSRa)	R_{800}/R_{680}	Blackburn 1998

2.7 Microscopy

Leaf tissue samples for histological analysis were taken from sporulating CLS lesions. Samples were fixed in 2.5% glutaraldehyde and 2% paraformaldehyde in 0.1 M sodium cacodylate buffer with pH 7.35 for 24 h (Karnovsky 1965). The tissue was dehydrated and embedded in Spurr resin (Spurr Low-Viscosity Kit, Merck KGaA, Darmstadt, Germany). Semi-thin sections were cut with a glass knife and stained with toluidine blue (0.1% aqueous). Light microscopy of stained samples was carried out using a Leitz DMR photomicroscope (Leica Microsystems). Macroscopic images of unprepared samples were recorded with a Leica MZ16 F stereo microscope (Leica Microsystems).

2.8 Statistical analysis

Statistical analyses were performed using SPSS 22.0 (SPSS Inc. Chicago, USA). Data were tested for normal distribution and equity of variances. The Tukey's honestly significant difference (HSD) test was used to separate subgroups and the means between two genotypes were compared using the t-test in case of a normal distribution, otherwise by the Mann–Whitney U-test. In all tests a significance level of $P = 0.05$ confidence was chosen.

3 RESULTS

3.1 Progress of Cercospora leaf spot disease depending on sugar beet genotypes

The sugar beet genotypes were selected based on their susceptibility to *C. beticola* described by the breeder KWS SAAT SE. To confirm the assessment of the breeder from the field, disease progress of the five genotypes Bv1+Q, Bv2-Q, Bv4_r, Bv6_s and Bv7_s was evaluated in experiments under greenhouse conditions (Figure 2). Genotypes Bv6_s and Bv7_s were highly susceptible. The first lesions appeared 9 days after inoculation (dai) on genotype Bv7_s and 10 dai on all other genotypes. The diseased leaf area increased within ten days up to 50% and 70% on Bv6_s and Bv7_s, respectively (Figure 2A). Disease was less severe on the other three genotypes. The genotypes Bv2-Q and Bv4_r showed lower percent diseased leaf area over time with an increase up to approximately 20%. Bv1+Q was the least infected genotype with only 10% diseased leaf area 19 dai. The number of CLS lesions per leaf increased on all genotypes continuously during the experimental time (Figure 2B). Bv6_s and Bv7_s had about two times more lesions than Bv4_r and even seven times more than Bv1+Q and Bv2-Q. Typical lesions appeared as well-defined depressions of the leaf surface on Bv6_s and Bv7_s and were approximately 4 mm² in size and considerably larger than on Bv1+Q, Bv2-Q and Bv4_r on the day of first appearance (Figure 2C). They grew by up to 2 mm² within the first three days and then reached final sizes varying from 5 to 6 mm² on susceptible genotypes and 3 to 4 mm² on resistant sugar beets, respectively.

In order to investigate the spore density of *C. beticola*, the number of conidia per diseased leaf area was assessed after two days of incubation under 100% RH (Figure 2D). With about 40 conidia per mm², the spore density was lowest on genotype Bv4_r, followed by that on Bv1+Q with 95 conidia/mm². Both genotypes were significantly different from the highly susceptible Bv6_s and Bv7_s, on which *C. beticola* produced 260 and 370 conidia/mm², respectively. The spore density was intermediate on genotype Bv2-Q.

3.2 Variation of lesion phenotypes on sugar beet genotypes

The typical CLS symptom was a circular, brown to red lesion with a gray center. However, the variation in lesion appearance among and within genotypes was high. Alternatively, lesions had a wide brown margin and small center or a large, dominating center with a thin margin. Every constellation in-between was possible. Furthermore, some lesions were uniform without visible segmentation into margin and center, and the color ranged from almost white over gray to brown, with or without reddish or brown margin (Figure 3 and 6). The lesion variability was investigated in detail in order to know whether lesion types are related to genotypic disease resistance. The CLS phenotypes were categorized based on the ratio of center to margin (Figure 3) and the frequency of lesion types on the sugar beet genotypes was assessed (Figure 4). On genotypes Bv1+Q, Bv2-Q and Bv4_r more than 50% of the lesions showed no differentiation into margin and center (class 0). About one third of the lesions had a smaller center than margin or the central and marginal areas had the same size (class 1). Only very few leaf spots had a larger center than margin. The genotypes with higher susceptibility to CLS (Bv6_s and Bv7_s) had a lower percentage of uniform lesions (13 and 18%) and more lesions with a ratio greater than 1 and up to 2. Roughly 15% of the lesions on Bv7_s had a predominant center with a size more than double the margin size.
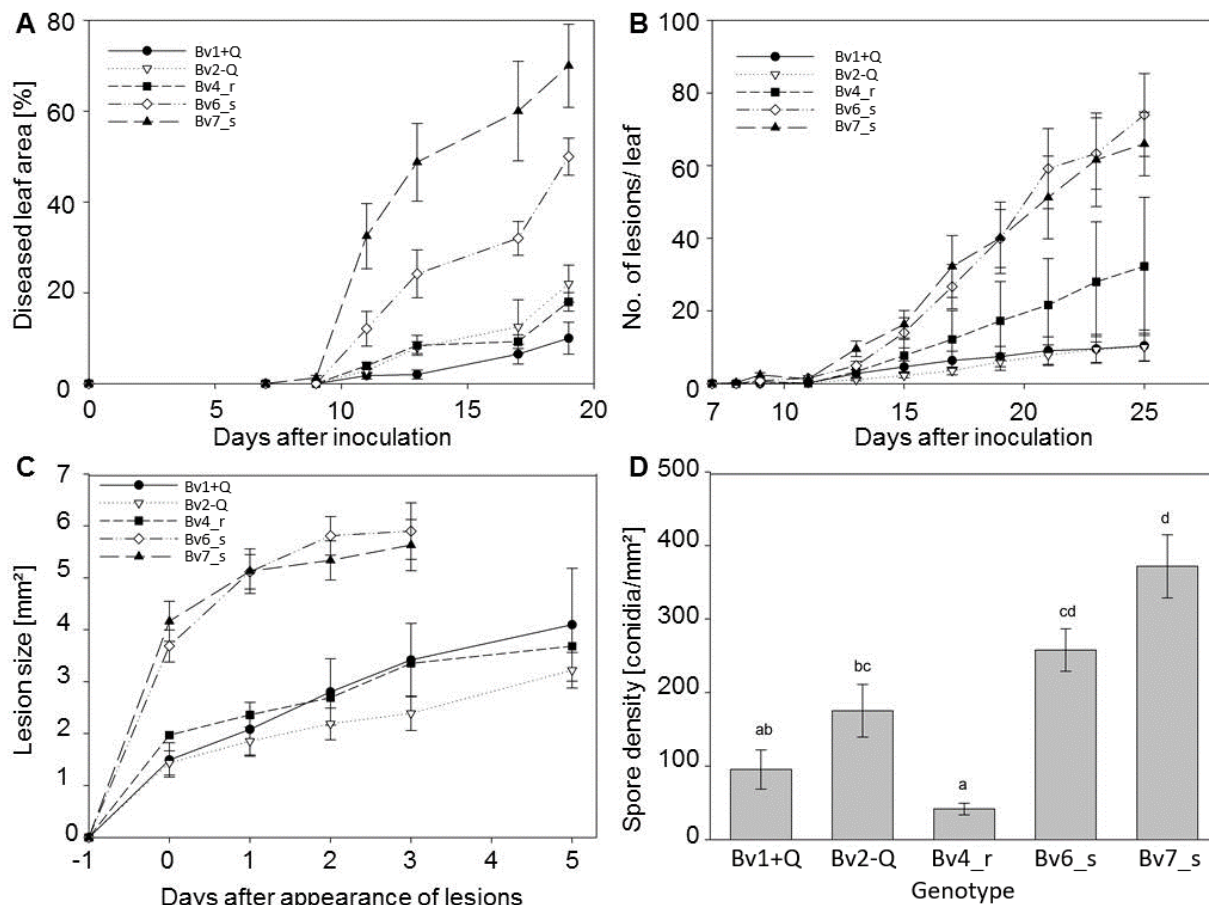
Figure 2: Assessment of Cercospora leaf spot (CLS) on sugar beet genotypes Bv1+Q, Bv2-Q, Bv4_r, Bv6_s and Bv7_s. (A) progress of leaf area covered with CLS within three weeks after inoculation (n=12 leaves). (B) number of CLS lesions per leaf starting from the day of appearance of the first lesions 9 dai (n=16 leaves). (C) size of developing CLS lesions within three days after their appearance (n=10 lesions). (D) spore density as the number of conidia per unit diseased leaf area after 2 days of incubation under 100% relative humidity (n=20 lesions); values with the same letter are not significant different (Tukey's HSD test, $P = 0.05$). Bars indicate standard error of the mean.

3.3 Spectral characterization of Cercospora leaf spot lesions

To see whether differences in CLS resistance can be characterized by HIS, spectral signatures of specific subareas of mature CLS lesions were manually extracted from hyperspectral images. Interestingly, the subarea-specific reflectance spectra on the genotypes were remarkably similar (Figure 5). Reflectance of the lesion margins was characterized by a decreased chlorophyll peak and an increased reflectance between 580 to 700 nm compared to spectra of non-infected tissue (Figure 5A and B). Additionally, the slope at the VIS-NIR transition (red edge) was less steep. Generally, reflectance of lesion centers was much higher in the VIS and NIR range than the spectra of the non-infected leaf tissue (Figure 5D).

8

With the spectral information from 400 to 900 nm it was possible to differentiate more explicit lesion subareas than only center and margin. A transition area between the margin and the center with an intermediate spectral signature could be identified on most genotypes (Figure 5C). For Bv4_r only two subareas could be detected. The comparison with the spectral signatures of the other genotypes indicated that spectral characteristics for the central area were absent on this genotype. Using the specific spectra as class reference spectra (endmembers), SAM classification was applied to the hyperspectral images (Figure 6). As visualized by the pseudo-color images, composition of lesions varied with the sugar beet genotype. In accordance with the visual segmentation (Figure 4), the size of lesion centers was extended on Bv6_s and Bv7_s and the transition area was more pronounced on Bv1+Q and Bv2-Q. For more details on the lesion characterization see publication 2 (Leucker *et al.* 2016).
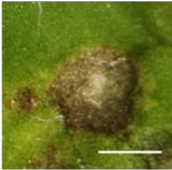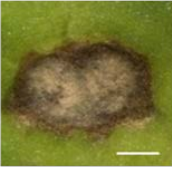
Class	Center to margin ratio	Examples
0	-	
1	$0 < x \leq 1$	
2	$1 < x \leq 2$	
3	$x > 2$	

Figure 3: Classes of Cercospora leaf spot lesions based on the ratio of center size to margin size. Exemplary lesions with corresponding center to margin ratio 21 days after inoculation. Scale bars represent 1 mm, x stands for the value of the ratio.

3.4 Spectral characterization of Cercospora leaf spot development

The development of CLS lesions on the sugar beet genotypes was analyzed in detail to identify the differences in resistance based on the resistance source. For more details on the investigations particularly focused on the differences in resistance based on the two QTL of genotype Bv1+Q compared to Bv2-Q see publication 3 (Leucker *et al.* 2017). Within an experiment, first visible changes appeared on all genotypes on the same day. Initial lesions on the genotype Bv2-Q, lacking the resistance QTL, and the highly susceptible Bv6_s appeared as depressions of the leaf surface, which still remained green. During further development, the tissue became necrotic brown with a white to grayish center. Over time the spectral reflectance of CLS lesions on Bv2-Q, Bv4_r and Bv6_s increased continuously in the VIS range, especially from 600 to 650 nm (Figure 7A). This increase was considerably higher for Bv2-Q and Bv6_s than for the resistant genotype Bv4_r. The NIR reflectance of the three genotypes decreased compared to the reflectance of healthy tissue directly at the day of lesion appearance. The lesions of the genotype Bv1+Q, carrying the resistance QTL, were characterized by a faster and more distinct increase of reflectance in the VIS range right from 9 dai (Figure 7A). The decrease in the NIR range was also stronger than on the other genotypes and only marginal changes were detected during the further experimental time. The initial lesions on Bv1+Q already appeared as brown, necrotic depressions and showed minor changes compared to lesions on the other genotypes (Figure 7B).
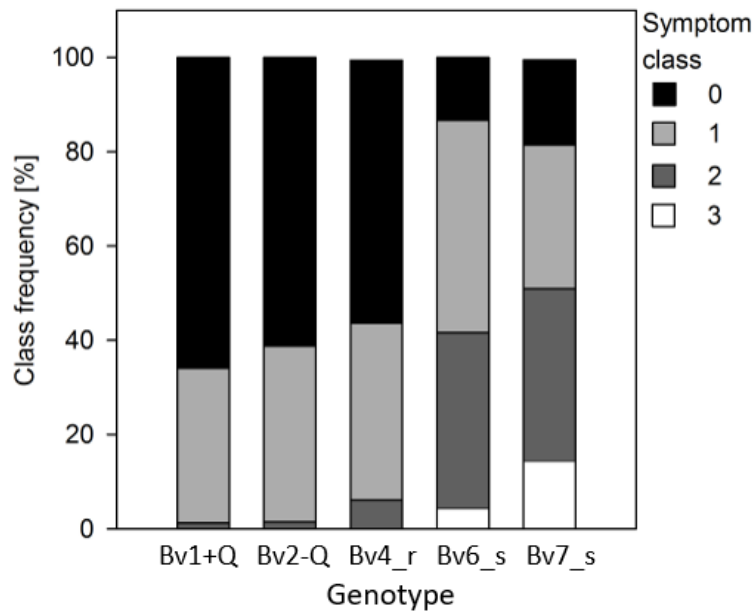

Figure 4: Frequency of four Cercospora leaf spot classes based on the center to margin ratio on five sugar beet genotypes differing in *C. beticola* susceptibility. The size of ad least 100 mature lesions on each genotype was measured 20 to 22 d after inoculation. When visible, lesion centers were measured, too, and the size of the darker margin was calculated as difference of total lesion area and central area. For details of lesion classes see Figure 3.

To validate the hyperspectral differences in disease development, spectral signatures of developing CLS lesions on Bv8 and Bv9 with the same resistance source as Bv1+Q and Bv4_r, respectively, were analyzed (Figure 8). Dynamics of spectral signatures on Bv8 resembled the development on genotype Bv1+Q (Figure 7 and 8). Reflectance in the VIS range increased right at the time of lesion appearance and stayed on this level during the measuring period. The development on Bv9 and Bv4_r were also comparable. A continuous increase of reflectance in the VIS region was observed. The shape of the signatures of Bv8 and Bv9 differed a bit and the reflectance was slightly higher on these two genotypes than on Bv1+Q and Bv4_r, nevertheless, the difference in development depending on the resistance source became clear.

3.5 Spectral characterization of sporulation of *Cercospora beticola*
The sporulation of *C. beticola* was related to the sugar beet genotype. To assess the spore production by HIS, spectra information before and after incubation were analyzed. Average reflectance spectra (from 400 to 900 nm) of non-sporulating CLS lesions on Bv1+Q, Bv2-Q, Bv4_r and Bv6_s were extracted 19 dai and compared to reflectance of non-infected tissue (Figure 9B). Spectral signatures of CLS were characterized by an increased reflectance from 400 to 700 nm and a decrease of the red shoulder. The increase in reflectance of the visible light was higher on genotypes Bv2-Q and Bv6_s than on the more resistant sugar beets Bv1+Q and Bv4_r.

The incubation of diseased plants under 100% RH for 2 d induced the formation of bundles of conidiophores spreading throughout the light center of the lesions on both sides of the leaves (Figure 9A and 10). The conidiophores protrude from darkly pigmented hyphal agglomerates (pseudostromata) and bear long, hyaline conidia. These alterations on the leaf tissue level led to a strong decrease in reflectance over the whole wavelength spectrum for all genotypes. The change in reflectance due to the incubation was strongest on the susceptible genotype Bv6_s. To evaluate differences between the genotypes the areas between the two spectral signatures 19 and 21 dai (indicated as gray area in Figure 9B) were calculated (Figure 9C). Interestingly, the values were significantly higher for Bv2-Q and Bv6_s than for highly resistant genotypes Bv1+Q and Bv4_r. For example, Bv6_s had values three times higher than Bv1+Q. To compare the spectral differences with the spore production of *C. beticola*, the number of conidia per lesion was counted. The gradation of the spore production on the different genotypes was similar to the spectral difference. Over 2000 conidia per lesion were produced on Bv2-Q as well as on Bv6_s. Compared to that, spore production was significantly lower with an average of 500 conidia per lesion on Bv1+Q and Bv4_r, respectively.

Spectral signatures of sporulating CLS lesions on Bv6_s were analyzed in more detail to evaluate the influence of the fungal spores and the melanized conidiophores. Spectral reflectance was measured from the side with focus on the spores as well as from above before and after removing the spores (Figure 11). The spectra extracted from the acicular spores showed a unique shape. The reflectance in the VIS range was considerably higher, especially around 500 nm. The increase in the NIR range was less strong compared to reflectance of CLS lesions. The removal of the spores had almost no influence on the reflectance from above. Apart from the NIR region, spectral signatures of the sporulating CLS lesions with and without spores were very similar.
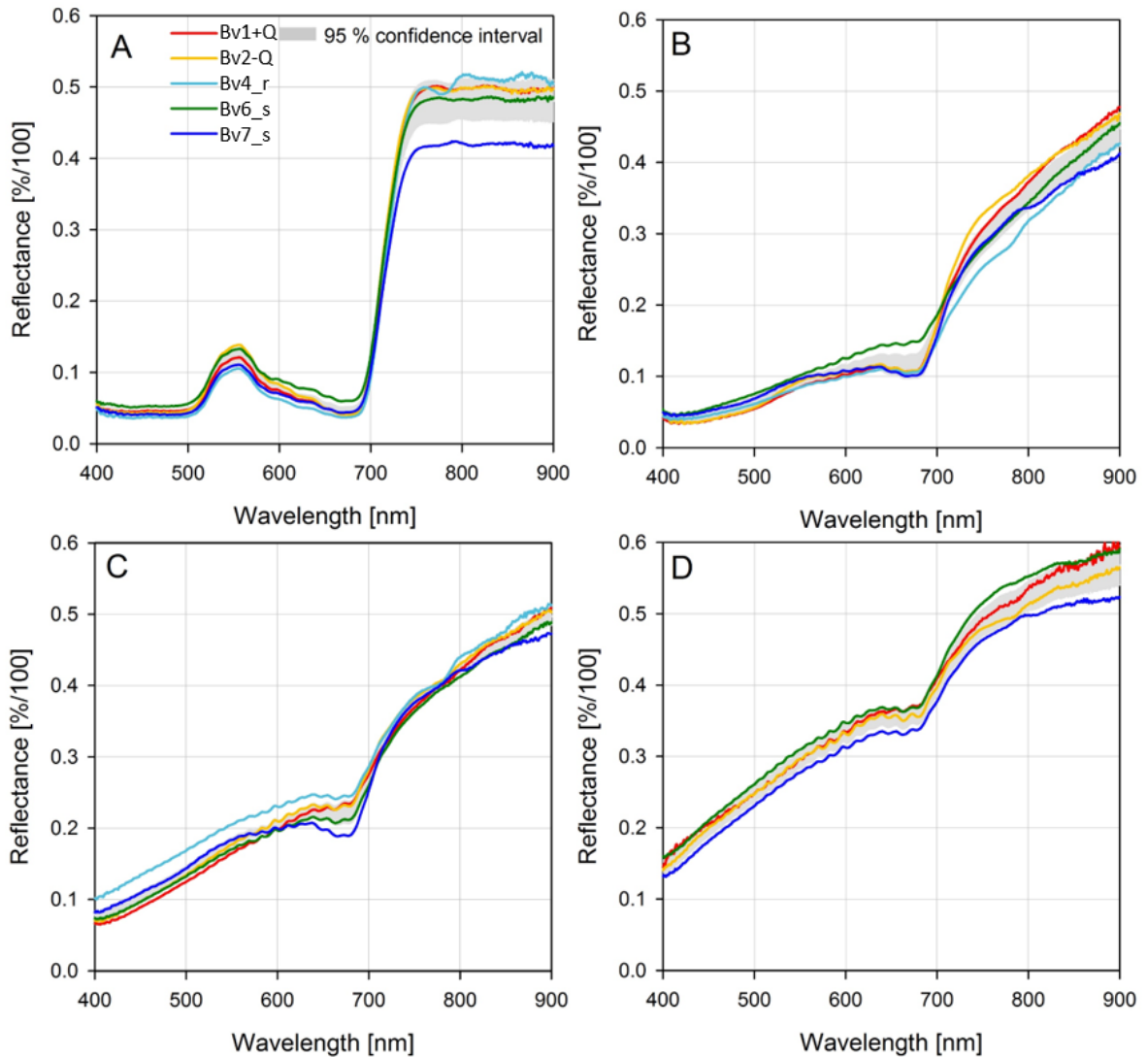
Figure 5: Comparison of the spectral signatures of (A) non-infected tissue and *Cercospora beticola* infected tissue of five sugar beet genotypes. Lesions were separated in three subareas (B) margin, (C) transition area and (D) center. Reflectance spectra represent the mean of n = 500 pixels each. The 95% confidence intervals for the mean of all genotypes are highlighted in gray.

3.6 Information content of hyperspectral reflection and transmission of Cercospora leaf spot infected leaves

To examine the additional information content of transmission measurements disease symptoms of a highly susceptible genotype were analyzed. CLS lesions on Bv6_s were well detectable in the RGB representations of both reflectance and transmittance data (Figure 12). The lesions were uniformly darker and mostly surrounded by a chlorotic halo in transmittance images. The calculation of the Cercospora leaf spot index (CLSI) resulted in a good differentiation between leaf tissue und CLS lesions for both, reflectance and transmittance. The transition from lesion to green leaf tissue was more blurred using reflectance values than transmittance. The pigment

12

specific simple ratio (chlorophyll a, PSSRa) resulting from reflectance data was highly influenced by leaf structure, however, various CLS lesions had a uniform composition. Using the transmittance data, the lamina was very homogenous and the veins were well separable. Furthermore, many differences between CLS lesions and also within lesions were detectable. The anthocyanin reflectance index (ARI) calculated from transmittance data provided a better differentiation between lesions, leaf tissue and veins, whereas differences between lesion margin and center were only visible on ARI reflectance images. The gray scale image of the photochemical reflectance index (PRI) was noisier than the other SVI for reflectance and particularly for transmittance.

In order to compare the SVI values of a CLS lesion, a transect through one lesion was extracted, exemplary for ARI and PRI (Figure 13). The ARI of the green, non-infected tissue for reflectance and transmittance was very similar, just below 0 (Figure 13A). Within the lesion, the ARI values increased considerably. The transmittance values of the lesion were three to eight-fold higher than the reflectance data. There were no clear differences between reflectance and transmittance for the PRI (Figure 13B). Apart from the outliers, both values decreased slightly from around 0 to approximately -0.1 within the CLS lesion.

Compared to the SVI, calculated from specific single wavebands, spectral signatures were analyzed over the whole wavelengths range from 400 to 1000 nm. The spectral signatures of non-infected leaf tissue extracted from reflectance and transmittance images showed some basic similarities: little reflectance and transmittance of blue and red light, a peak in the green range and a steep increase in the NIR region (Figure 14A). The shape of the reflectance signature was flatter in the visible region than that of the transmittance. Spectral signatures of CLS lesions differed depending on the region of the lesion. The reflectance of the visible light increased from the lesion margin to the center continuously; in contrast, the transmittance decreased in the green to red range towards the lesion center. The decrease of the red shoulder around 700 nm was considerably more distinct in the transmittance spectra. Consequently, the absorption of the VIS and NIR radiation was higher in the marginal area of the CLS lesions and was decreasing towards the central region. The non-infected tissue showed highest absorption (Figure 14B).

Subtracting spectral signatures of non-infected areas from lesion center or margin (= difference spectra) identified also clear differences between reflectance and transmittance (Figure 15). In the region of the green peak and the red shoulder transmittance spectra showed greatest differences (up to 30%). Transmittance of the lesion center was remarkably lower than transmittance of the margin. The calculated differences of reflectance spectra were smaller. Reflectance of the central area differed in the VIS and NIR region. Reflectance of marginal area diverged more in the NIR range.
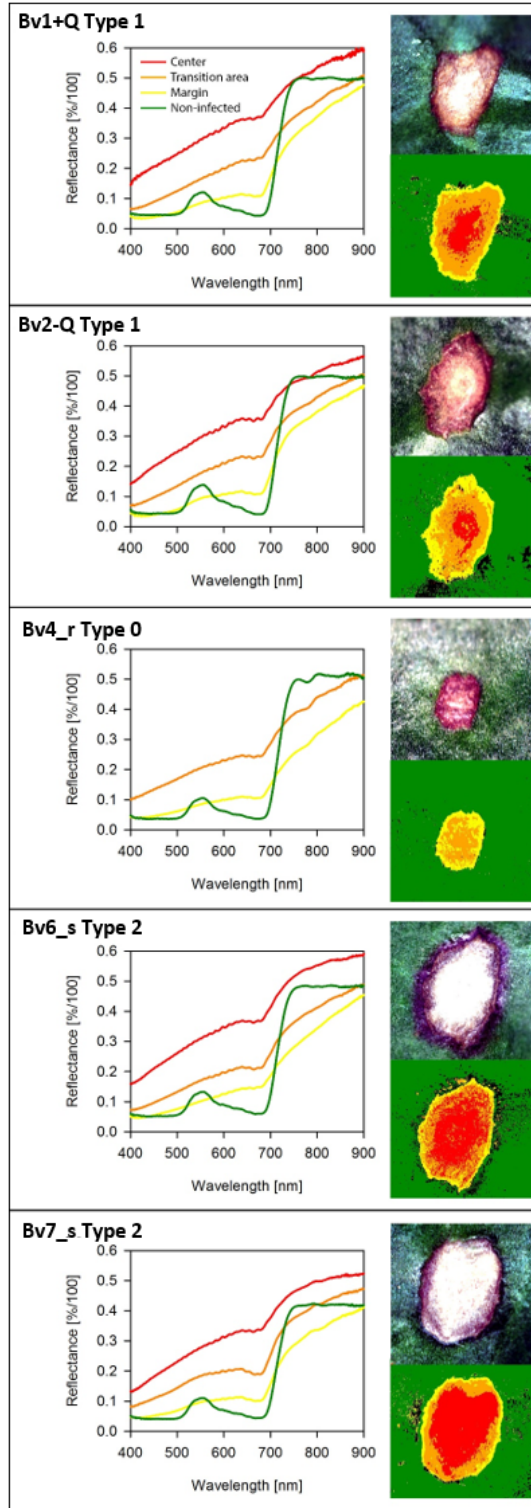
Figure 6: Spectral signatures of Cercospora leaf spot (CLS) lesion subareas (left) and Spectral Angle Mapper (SAM) classification based on these reference spectra. RGB images of CLS lesions of indicated class (upper right panels) and pseudo-color image of SAM classification result (lower right panels) for sugar beet genotypes Bv1+Q, Bv2-Q, Bv4_r, Bv6_s and Bv7_s. Black pixels were not classified.
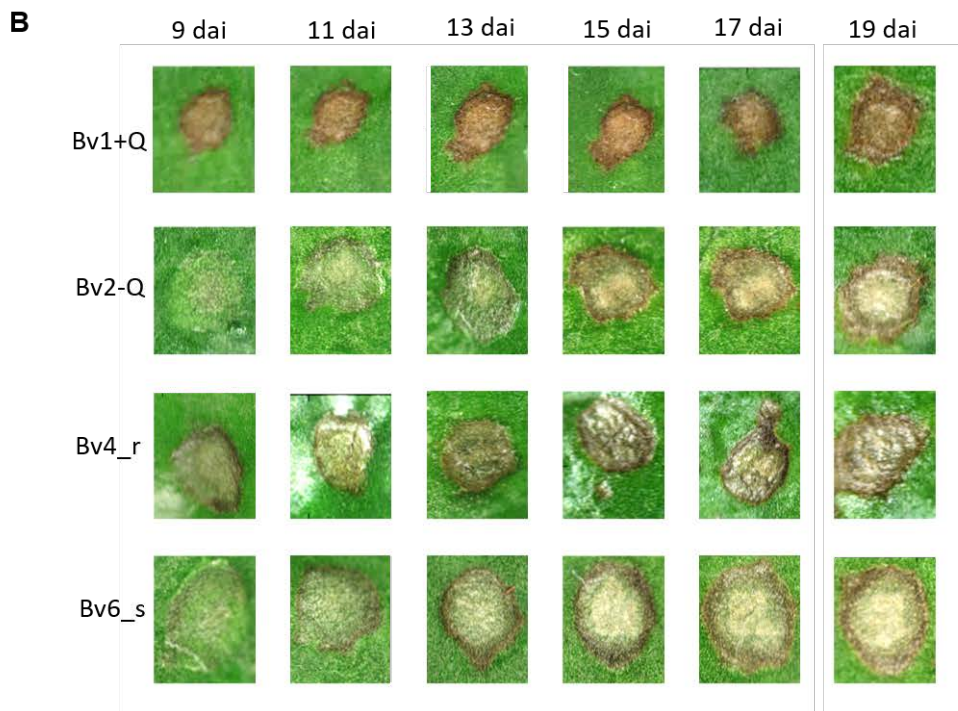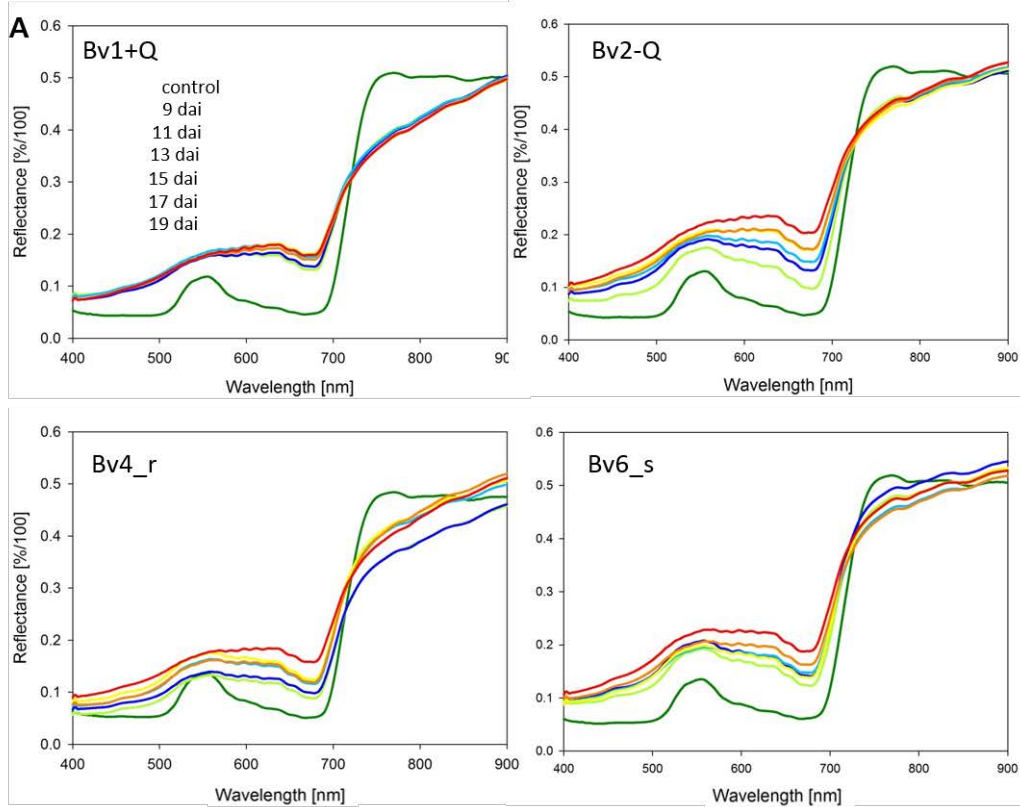
Figure 7: (A) Spectral signatures and (B) RGB images of sugar beet genotypes Bv1+Q, Bv2-Q, Bv4_r and Bv6_s non-inoculated (control) and 9 to 19 days after inoculation (dai) with *Cercospora beticola*. Reflectance spectra represent the average of n = 10 lesions with at least 8000 pixels each.

Figure 8: Spectral signatures of sugar beet genotypes Bv8 and Bv9 non-inoculated (control) and 14 to 24 days after inoculation (dai) with *Cercospora beticola*. Reflectance spectra represent the average of n = 10 lesions with at least 8000 pixels each.
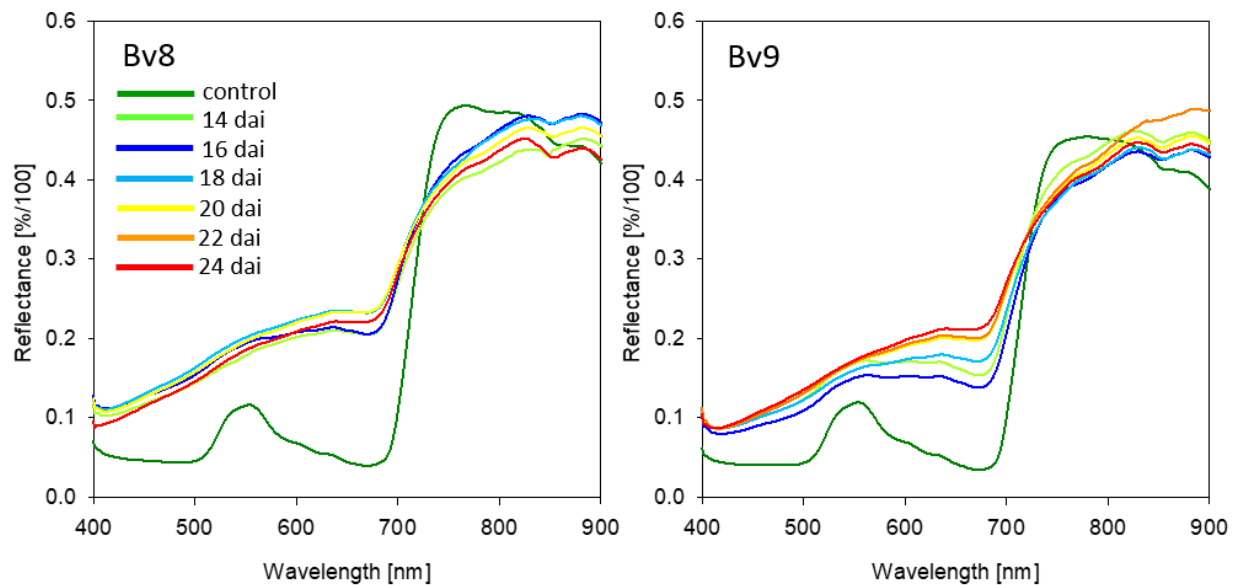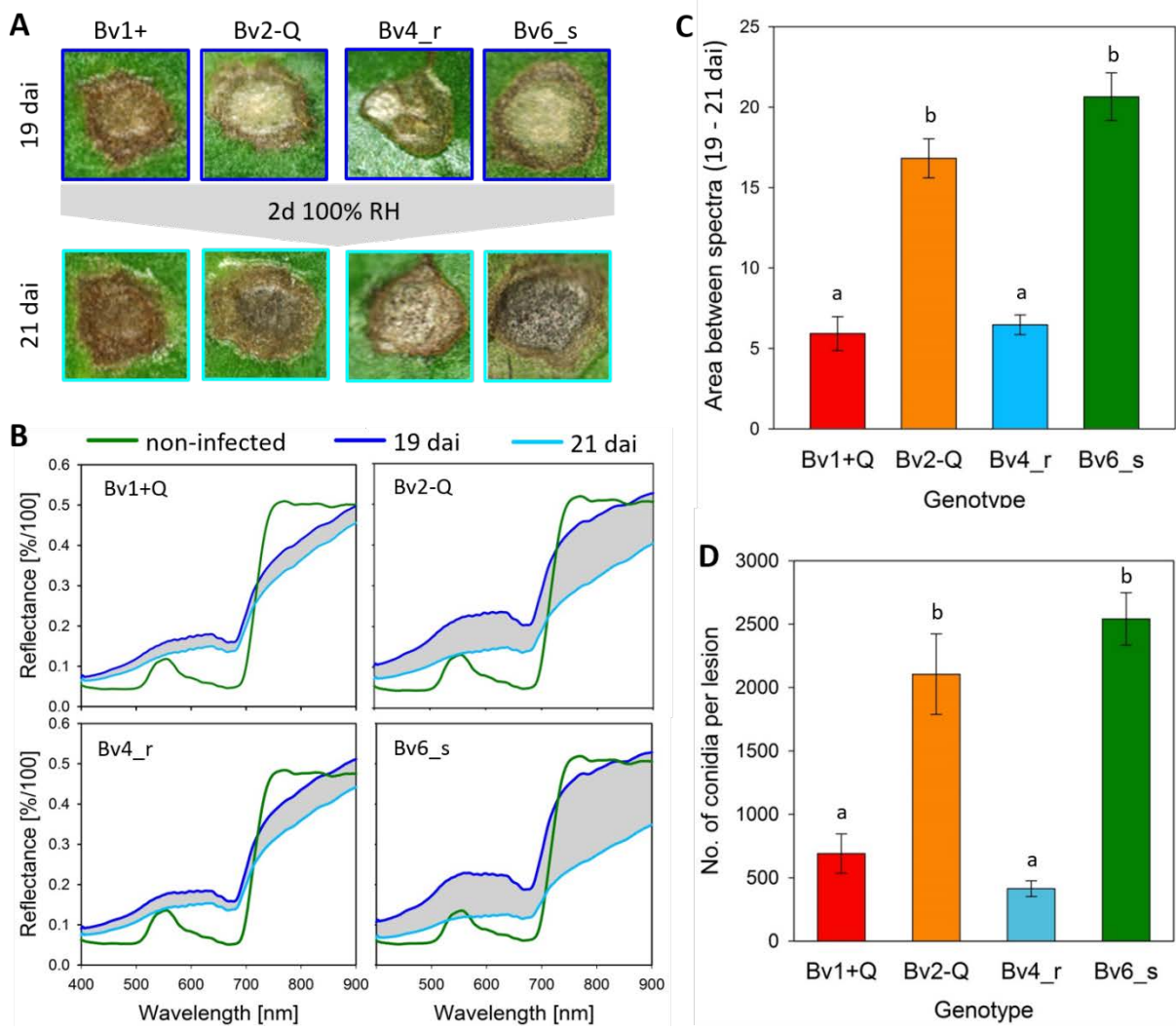
Figure 9: Sporulation of *Cercospora beticola* induced by incubation under 100% relative humidity (RH) for 2 days. (A) RGB images of Cercospora leaf spot (CLS) lesions on four sugar beet genotypes differing in *C. beticola* resistance before (19 days after inoculation; dai) and after (21 dai) induction of sporulation. (B) spectral signatures of heathy control and CLS lesions. (C) area between spectra with and without sporulation. (D) average number of conidia per lesion; values with the same letter are not significantly different (Tukey's honestly significant difference test, $P = 0.05$, $n \geq 20$). Bars indicate standard error of the mean.
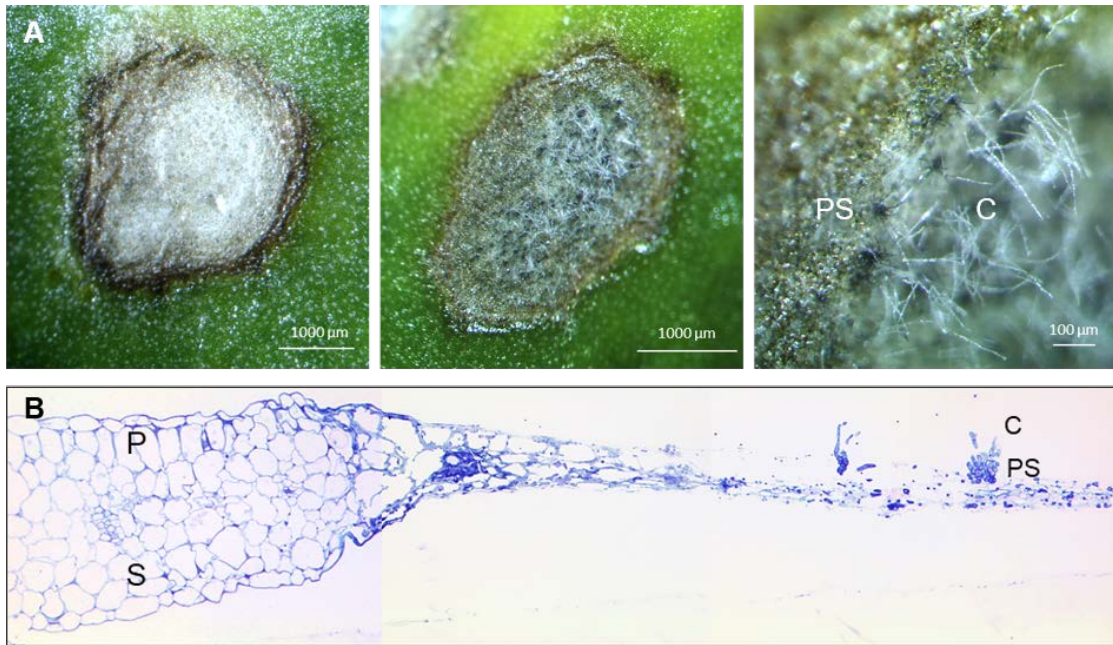
Figure 10: (A) Cercospora leaf spot (CLS) lesions on the susceptible sugar beet genotype Bv6_s 19 days after inoculation (dai; left) and after incubation under 100% relative humidity for 2 days (center and right; 21dai). The incubation induced the formation of dark conidiophores protruding out of the leaf surface and carrying long, hyalin conidia. (B) Thin-sections of CLS lesion on a sugar beet leaf stained with toluidine blue. Leaf tissue without macroscopic symptom (left), symptomatic necrotic tissue (middle) and conidiophores in the center of the lesion (right). Healthy leaf structure with palisade parenchyma (P) on the upper and spongy parenchyma (S) on the lower leaf side. Pseudostroma (PS) with protruding conidiophores (C) may arise on both leaf sides.

4 DISCUSSION

There are several ways to assess disease severity of CLS on sugar beets, but mostly it is rated based on the average percentage of infected leaf area (Rossi *et al*. 1999; Wolf and Verreet 2002). Disease progress results from the combination of an increase in the number of leaf spots and in the size of lesions. In the experiments, the period of lesion growth was limited to 3 – 5 days, whereas the increase in lesion number was observed for more than two weeks after the appearance of the first leaf spots. The initial lesion diameter was related to host plant resistance indicating an inhibition of pathogen colonization. The host plant resistance had no significant effect on the time until the appearance of the first lesion(s). Under controlled conditions, where no sporulation was induced, the increase of lesion numbers with time could not be due to a new infection cycle. Differences in the time until appearance of the lesions on the same genotype could result from a longer period of time until spore germination or delayed growth of some germ tubes and hyphae (Feindt *et al*. 1980; Rossi *et al*. 2000).

The lower infection rate of resistant sugar beet genotypes is in accordance with the report of Rossi *et al*. (1999). They also observed a reduced number of leaf spots on resistant cultivars and significantly larger lesions on susceptible sugar beets. Furthermore, sporulation on a resistant genotype was reduced to 35% (Rossi *et al*. 2000). Similar host-pathogen relationships were observed in barley infected by *Cochliobolus sativus*. Fetch and Steffenson (1999) distinguished varying host-pathogen compatibility of spot blotch based on the type and relative size of lesions. Differences in components of rate-reducing resistance such as reduced sporulation were also described in the peanut and *Cercospora arachidicola* interaction (Ricker *et al*. 1985).
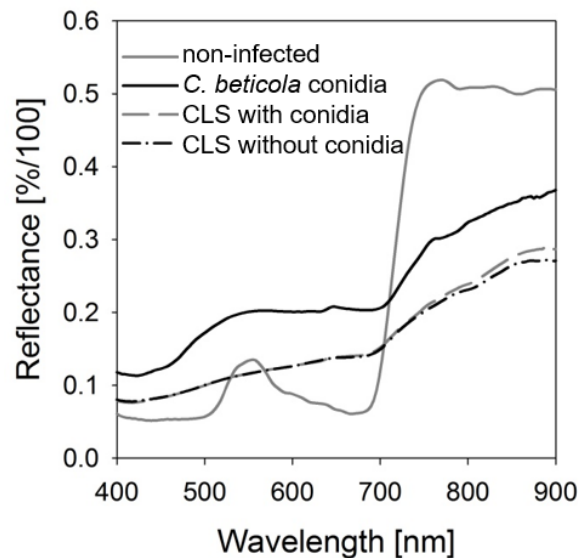

Figure 11: Spectral signatures of non-infected plant tissue and sporulating Cercospora leaf spot (CLS) lesion on susceptible sugar beet genotype Bv6_s 21 days post inoculation. Hyperspectral images of lesions were taken from the side with focus on the spores as well as from above before (CLS with conidia) and after removing the spores (CLS without conidia).
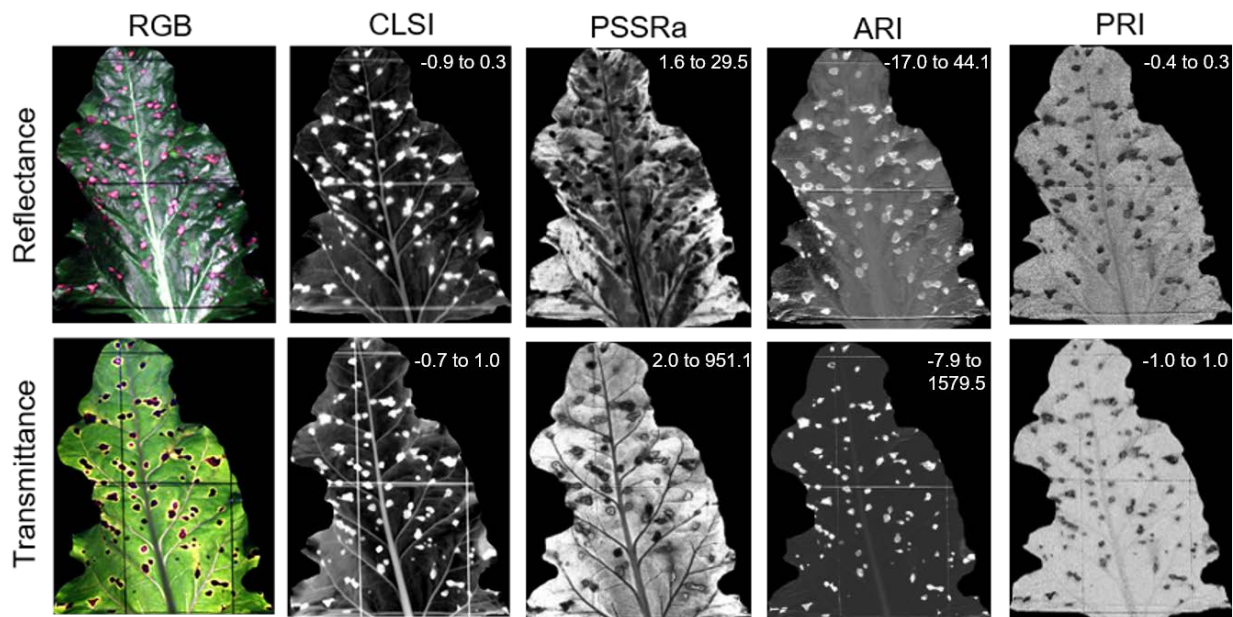
Figure 12: RGB and gray scale representations of spectral vegetation indices of a sugar beet leaf infected by *Cercospora beticola*. Cercospora leaf spot index (CLSI), pigment specific simple ratio (chlorophyll a, PSSRa), anthocyanin reflectance index (ARI) and photochemical reflectance index (PRI) were calculated from hyperspectral reflectance and transmittance images. Light-colored pixels indicate high index values and dark pixels low values with given value range (upper right corner).

Niks and Kuiper (1983) described reduced infection success accompanied by impaired growth and development of rust colonies on partially resistant barley. Infection types may also vary within categories from low to high even in qualitative resistance (of wheat and barley) to races of rust fungi (Parlevliet 1976; Kolmer 1996).

The categorization of the different lesion types based on the ratio of center to margin and the frequency on the different genotypes implied a tendency from no lesion centers (high resistance) to larger centers (high susceptibility). The larger centers might be associated with the significantly higher spore production on genotypes Bv6_s and Bv7_s, because conidiophores are produced in this central area (Weiland and Koch 2004). The resistant genotype with the lowest spore density showed no lesion centers in the spectral analysis. Decreased spore production is one critical component of quantitative resistance against polycyclic diseases that delays disease epidemics as, for example, in barley cultivars resistant to *Puccinia hordei* and in peanuts resistant to *C. arachidicola* (Parlevliet 1979; Foster *et al*. 1980).

Analysis of symptom phenotypes has the potential to give insights into the physiology of the host-pathogen interactions (Mutka and Bart 2015). The sugar beet genotypes differing in resistance to *C. beticola* exhibited several CLS phenotypes per genotype. It was observed in all experiments that the lesions on the resistant genotypes had mostly smaller centers than those on the susceptible ones. This phenomenon is probably the consequence of the individual host-pathogen relationship. The result of the interaction is based on the genotype of both organisms and the ambient conditions. Ruppel (1972) characterized fourteen *C. beticola* isolates which varied in morphology *in vitro* and in virulence. However, differences in disease severity among sugar beet

lines were highly significant in all tests and the host resistance examined was effective against all isolates. The well described, race-specific resistance in sugar beet against the isolate C2 plays hardly any role in the field (Duffus and Ruppel 1993; Weiland and Koch 2004). Breeders aim at a broad-spectrum resistance against all populations of a pathogen under various environments.

The spectral characterization of CLS revealed that reflectance varied within lesions. Four spectral signatures could be extracted along a transect from healthy green tissue to the center of the diseased tissue. These signatures differed from each other in explicit regions of the electromagnetic spectra. The increase in the reflectance in the VIS range was particularly characteristic for the transition area and the center, whereas the differences in the margin specific signature were more pronounced for the decrease of the NIR reflectance shoulder. Kuska *et al*. (2015) have shown that the VIS reflectance of barley leaves increased as powdery mildew colonies develop. A decrease of the NIR reflectance at 800 nm was also reported for the chocolate spot disease on *Vicia faba* caused by the necrotrophic fungus *Botrytis fabae* (Malthus and Madeira 1993). Previous studies on HSI of disease symptoms on sugar beet have reported the same specific reflectance spectra of CLS centers and margins without focusing on the host genotype (Mahlein *et al*. 2012). They described the continuously changing reflectance along transects through lesions and over time.

Based on the specific signatures, lesions on sugar beet genotypes differing in CLS resistance could be differentiated into up to three subareas and the spatial proportions could be quantified. The composition of the CLS lesions, visualized by SAM classification, was directly related to the resistance of the genotype. Results from microscopic investigations focusing on the cellular structure of diseased leaves supported the differentiation of lesion subareas. Steinkamp *et al.* (1979) described three different areas in transmission electron microscopic studies of *C. beticola* lesions. The necrotic center was characterized by many hyphae and callose-like cell wall thickenings. According to Steinkamp *et al*. (1979), all cells within this area had collapsed and were necrotic, thus photosynthetic pigments had been degraded and therefore the absorbance of visible light increased. The degree of tissue degradation and the availability of nutrients for the pathogen may influence fungal growth and sporulation, thus possibly explaining the limitation of conidiophores to the center. *C. beticola* produces toxins to damage and colonize the host tissue (Daub and Ehrenshaft 2000). The photosensitizer cercosporin, for example, is an essential pathogenicity factor of *C. beticola* (Staerkel *et al*. 2013). The reduced lesion center size on resistant sugar beets may be due to a higher tolerance to this pathotoxin. Furthermore, a boundary zone separating the diseased tissue from healthy leaf tissue has been identified by Steinkamp *et al*. (1979). This boundary zone was divided into an inner and outer region. The inner zone was characterized by necrotic cells with thickenings of the inner surface of their cell walls. Fungal hyphae invaded this region, but not the outer zone, where electron-dense material was present in the intercellular space. The two characteristic zones may correspond to the transition area and the margin as identified spectrally in this study. Interestingly, Feindt *et al*. (1981) hypothesized that the boundary zone of CLS lesions on susceptible sugar beets resemble the complete infection site on resistant genotypes. This is consistent with the finding that resistant genotypes had a considerably higher portion of lesions with no or smaller centers than susceptible genotypes. The prevailing symptom phenotype on sugar beet genotype Bv4_r lacked the SAM class 'center'. It remains to be determined whether the reactions in the tissue of the lesion margin play a role in pathogen defense.
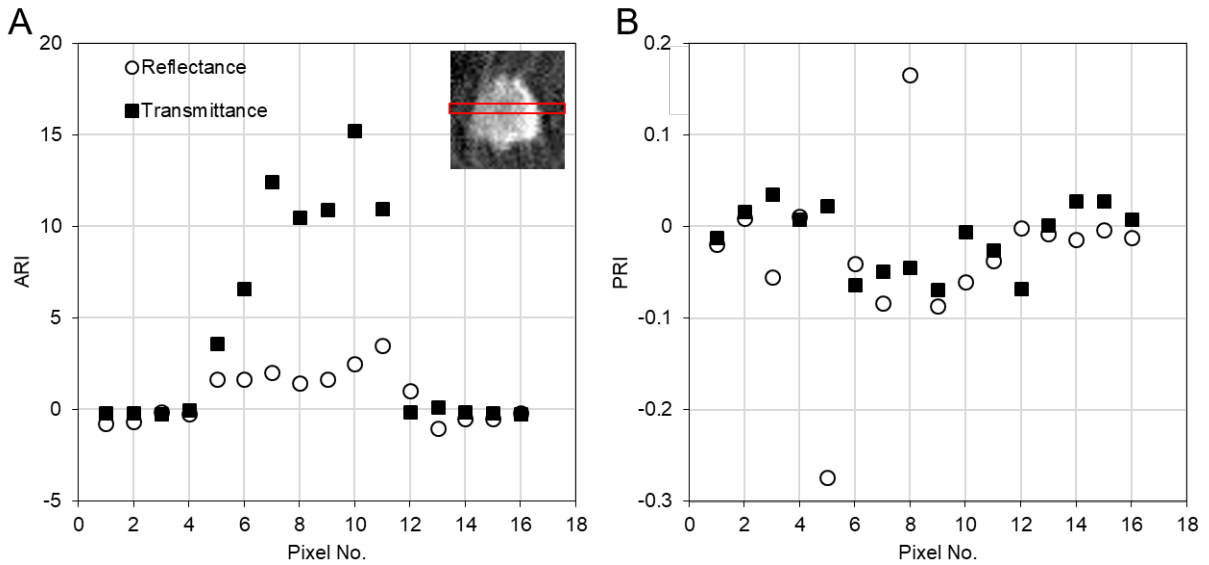
Figure 13: (A) Anthocyanin reflectance index (ARI) and (B) photochemical reflectance index (PRI) transects through a Cercospora leaf spot (CLS) lesion (see gray scale image) calculated for reflectance and transmittance data. Gray scale image illustrates transect through a CLS lesion where 16 ARI and PRI values were obtained.

Differentiation of lesion phenotypes based on subareas was improved by analyzing spectral signatures and has the potential to accelerate the screening process in breeding for CLS resistance. Apart from the different lesion phenotypes, the dynamics of spectral signatures of CLS were considerably different on the sugar beet lines. Differences based on the resistance source (Bv1+Q/Bv8 and Bv4_r/Bv9) or the presence of two QTL (Bv1+Q – Bv2-Q) were detectable. On all genotypes, the reflectance of the red shoulder declined at the time of lesion appearance and then remained at this level. This decrease in reflectance was much stronger on the resistant genotype Bv1+Q carrying the two QTL. Absorption in the far-red region is associated with brown pigments and phenolic compounds (Peñuelas and Filella 1998). A decreased reflectance in the NIR is also related to structural discontinuities, therefore indicating a higher degree of tissue damage on the resistant genotype Bv1+Q. In the early stage of lesion development, the leaf tissue collapsed in a limited area, presumably because of a decreased turgor pressure and the loss of membrane integrity possibly induced by cercosporin and other toxins (Daub and Ehrenshaft 2000; Goudet *et al.* 2000).

The appearance of the early lesions differed on the investigated genotypes. Whilst the collapsed tissue was still green on Bv2-Q and Bv6_s until 13 dai, the lesions on Bv1+Q had become brownish immediately. This and the initial higher increase of reflectance in the VIS on the QTL-carrying genotype indicate a stronger reaction of the affected cells compared with the continuous increase on the other genotypes lacking the resistance QTL. The increased reflectance in the VIS range is a consequence of reduced absorption by photosynthetic pigments and related to pigment degradation and decreased photosynthetic activity (Merzlyak *et al.* 1999). A slower reduction in photosynthetic activity of the susceptible genotypes may contribute to a better and persistent assimilate supply for the pathogen compared with the resistance interaction. In barley, even a localized increased photosynthesis rate of leaf tissue infected with the biotroph rust fungus *Puccinia hordei* was reported (Scholes and Farrar 1986). The abrupt increase of reflectance in the

22

VIS region on the resistant genotype Bv1+Q may be based on an enhanced sensitivity to cercosporin or a faster and stronger induction of defense mechanisms like lignification or phytoalexin production (Martin 1977; Daub and Ehrenshaft 2000). The resistance QTL seemed to enhance the reaction of the genotype Bv1+Q resulting in a limited CLS lesion development. On genotype Bv4_r and Bv9, disease progress appeared to be decelerated. The slow increase of reflectance in the VIS range ended at a similar level as measured on Bv1+Q, but the decrease of the red-shoulder was weaker.
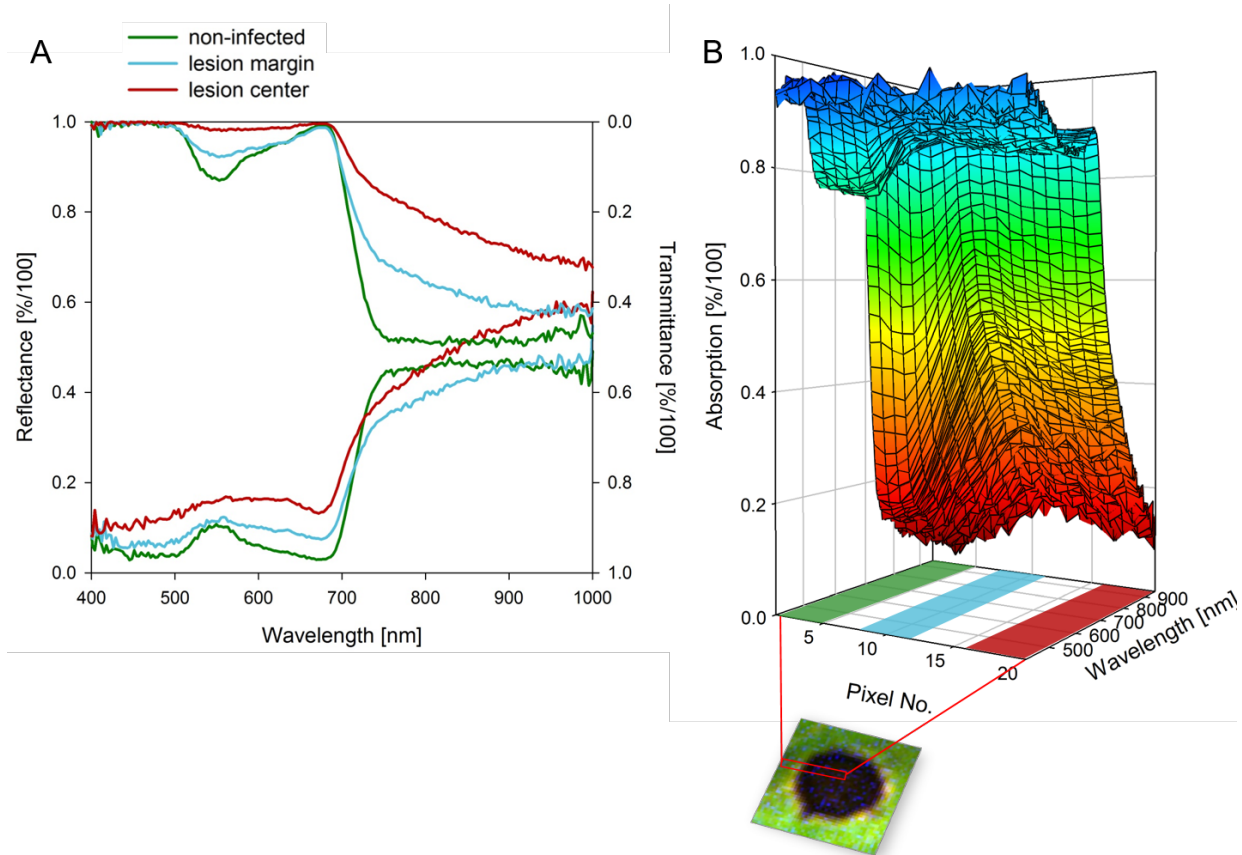
Figure 14: Reflectance, transmittance and calculated absorption spectra of non-infected leaf tissue and Cercospora leaf spot (CLS) lesion. Hyperspectral signatures were extracted (A) as average for non-infected-tissue (green), lesion margin (blue) and center (red) or (B) pixel-wise from a transect through characteristic leaf tissue as seen in the RGB representation from reflectance and transmittance images each. The absorption was calculated as 1 – (reflectance + transmittance).

Figure 15: Difference spectra of Cercospora leaf spot lesion margin and center for (A) reflectance and (B) transmittance values. Differences were calculated by subtracting spectral signatures of non-infected tissue from lesion center or margin.

Plants have evolved mechanisms to defend themselves against attacking pathogens. Numerous genes in pathogen recognition, cell signaling and defense-related proteins e.g. with ch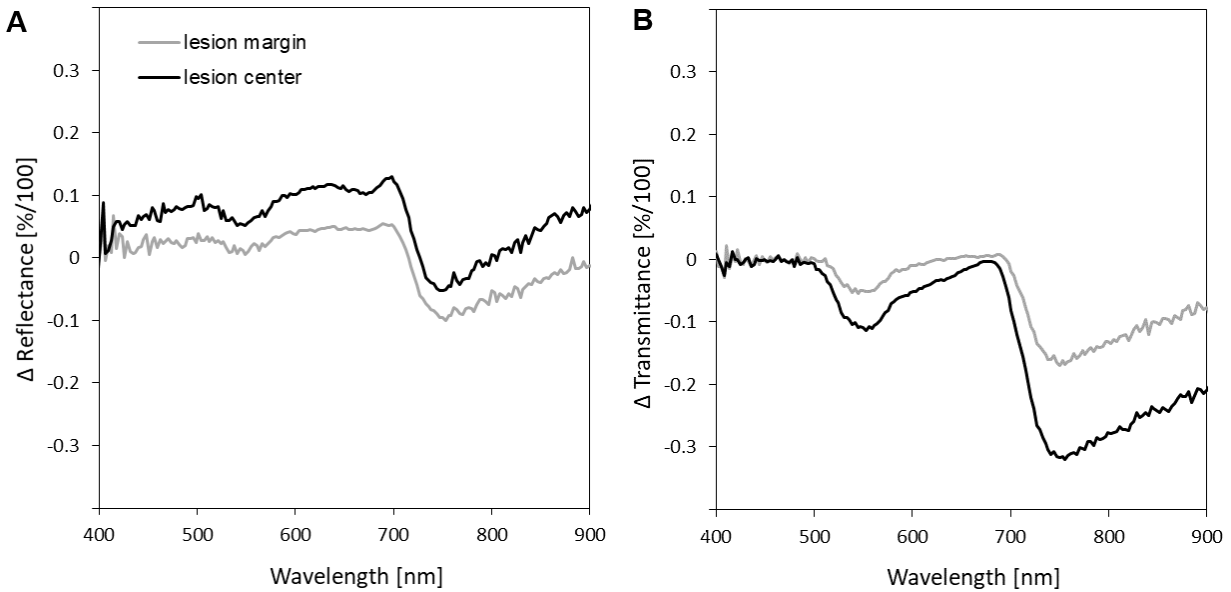itinase or glucanase activity are involved in quantitative resistance against *C. beticola* (Nielsen *et al.* 1997; Gottschalk *et al.* 1998; Weltmeier *et al.* 2011). In a transcription analysis, Weltmeier *et al.* (2011) found that polygenic (quantitative) resistance was characterized by higher induction of defense-related genes and a stronger defense response in the stage of formation of necrotic lesions than in the susceptible interaction. In order to inhibit pathogen growth, plants produce and accumulate phytoalexins which are synthesized *de novo* after pathogen infection. Geigert *et al.* (1973) isolated the isoflavone betavulgarin from sugar beet leaves infected with *C. beticola*. Betavulgarin inhibited mycelial growth drastically and resistant cultivars generally produced higher concentrations of betavulgarin in CLS lesions than more susceptible cultivars (Johnson *et al.* 1976; Martin 1977). An accelerated phytoalexin accumulation may be involved in the limited lesion development on the resistant genotypes.

In contrast, pathogens try to circumvent or inhibit plant defense. Schmidt and colleagues (2004, 2008) assumed that *C. beticola* suppresses the plant defense by abscisic acid (ABA) accumulation which led to a reduction of phenylalanin ammonium lyase (PAL) expression and activity. Moreover, ABA treatment has been shown to inhibit phytoalexin accumulation in potato (Henfling *et al.* 1980). Further investigations are needed to reveal details of the mechanisms of CLS resistance which are more difficult to investigate and to understand because of the long asymptomatic (latent) period of CLS compared with e.g. downy and powdery mildews (Oerke *et al.* 2006; Mahlein *et al.* 2012; Wahabzada *et al.* 2015). For instance, the resistance of barley to *Blumeria graminis* f.sp. *hordei* largely depends on the tissue reaction within 48 h after inoculation (Hückelhoven and Panstruga 2011), thus HSI approaches enable an identification of resistant genotypes within the first days after inoculation (Kuska *et al.* 2015).

24

The assessment of sporulation of *C. beticola* by HSI was investigated, because this epidemiologically relevant parameter allowed a good differentiation of the genotypes. In contrast to other leaf diseases of sugar beet, *C. beticola* starts spore production only under suitable environmental conditions. Due to that, sporulation could be induced synchronously when lesions were fully developed on all genotypes 19 dai. On susceptible plants, CLS lesions had produced more spores after 2 days than lesions on resistant genotypes. Since spores have not been removed within this time, probably more conidiophores had been formed on the susceptible genotype. The lesions with larger centers resulted in an increased reflectance before incubation. The dark pigmented conidiophores had a reducing influence on the CLS reflectance. In comparison, the spore layer above the leaf (lesion) surface had only marginal effects on reflection. The greatest changes in coloration and structure were found on the susceptible genotype leading to a stronger decrease of the spectral signature than on the resistant genotypes. Consequently, the differences between the spectral signature before and after incubation were closely connected to the number of conidia produced per lesion. So, the spectral difference may be used as proxy for the fungal spore production.

This newly developed approach is based on the hyperspectral microscope using a higher magnification compared to imaging systems on canopy or leaf level (West *et al*. 2003; Mahlein *et al*. 2012). Mostly, these systems were used to detect and quantify plant diseases or to characterize disease development. The presented approach assessed the fungal spore production as important resistance parameter for the first time by HSI. In the complex plant-pathogen interaction it might be helpful to analyze the different subprocesses of the host-pathogen interaction. The ability to reduce the fungal sporulation is an essential component of quantitative resistance that delays the diseases spreading and epidemic development (Bleiholder and Weltzien 1972; Rossi *et al*. 2000). This is, for example, also reported for peanuts resistant to *C. arachidicola* or barley cultivars resistant to powdery mildew (Foster *et al*. 1980, Asher and Thomas 1984). As selection for CLS resistance is mainly based on the visually assessed diseased leaf area in field trails, a closer view on the sporulation may be valuable for finding small positive effects (Wolf and Verreet 2005). Weiland and Koch (2004) argued that neighboring effects in breeding lines trials will probably occur and that the constant inoculum release will lead to an underestimation of varieties with major effects on the sporulation. To incorporate the quantification of the spore production into the breeding programs a reliable and effective assessment method is necessary. However, the measurement of spores is laborious and therefore it has not been used routinely as a selection method in sugar beet breeding, as far as currently known. Molecular bioassays which quantify fungal biomass as described by De Coninck *et al*. (2012) would fail to distinguish between mycelium and spores. Based on the presented findings, a phenotyping procedure based on HSI may be used to approximate the fungal sporulation under controlled conditions.

Reflection measurements have shown to be a valuable tool in plant characterization, although the part of absorbed and transmitted electromagnetic radiation is not known. To see whether transmittance data provide beneficial information, an HSI setup, measuring reflection and transmission of leaves, was developed. Spectral data of healthy and infected leaves of the susceptible genotype Bv6_s were analyzed and compared. The spatial lesion analysis was feasible due to the high resolution of the reflectance and transmittance images. Exposure time and focus could be optimized for both cameras, separately. For a more comprehensive study of different CLS lesions for example on different host genotypes, the matching of the exact pixels of reflectance and transmittance images must be improved in further work. So far, it was done manually and should be automated and more precise for an accurate calculation of absorbance. The

normalization relative to a white reference measurement may be optimized, too. It was done with two different references: a 100% white reflection standard and a 50% diffuser transmission sheet. In general, both measurement techniques had some disadvantages. Injuries or cracks of the leaf tissue, where the light got directly into the transmission camera, led to an oversaturation of the sensor. The value ranges of the SVI of the transmittance images were very large and some pixels had unusually high values. In the reflectance images, some very bright leaf veins led also to an oversaturation. It is possible that specular reflections on some parts of the leaf influenced image analysis as the information value of directly reflected light is low.

Another HSI technique for reflection and transmission is the HyperART system (Bergsträsser *et al*. 2015). It uses mirrors to measure the transmission of whole leaves with the same camera as for reflectance, but the mirrors may cause a certain distortion of the signal. Bergsträsser and colleagues could show that the combination of reflectance and transmittance improved the classification of CLS which may be used for monitoring disease development for example. Thomas *et al*. (2016) demonstrated that the transmittance provided additional information on the spatial differences of powdery mildew symptoms and necrosis. The yellowish halo surrounding CLS lesions is one example for an effect which is obvious in transmittance and not in reflectance images supporting the potential benefit of transmission measurements.

Interestingly, differences between the spectral signatures of non-infected leaf tissue were found for the measurement of reflectance and transmittance. The spectral signatures of the healthy sugar beet tissue published by Bergsträsser *et al*. (2015) were also slightly different. The anatomy of bifacial leaves is optimized to absorb the maximum of the photosynthetically active radiation. The energy of mainly blue and red light is absorbed and used for photosynthesis (Jacquemoud and Ustin 2001). The densely packed palisade parenchyma on the adaxial leaf side allows a certain portion of light to pass through. In the spongy mesophyll, where the cells are irregularly shaped and surrounded by air spaces, light is reflected and refracted on the different interfaces (air – water – cells). This increases the length of the light path within the leaves considerably (Richter and Fukshansky 1996). Light that is recorded by transmission measurements had passed all leaf layers and effects may be summed up along the path. Small changes in pigment content or composition of other metabolites in the leaf tissue are more likely revealed than using reflectance measurements. The presented results show that transmission measurements indeed provide additional information to the reflection. The effects seen in transmittance data were sometimes stronger than in reflectance data. This was the case for vegetation indices such as the ARI.

The analysis of the spectral signatures of lesion subareas revealed partly opposite information contents. Compared to the non-infected tissue, reflectance of lesion center was higher and transmittance lower. In the lesion margin, both, reflectance and transmittance of the NIR range decreased and led to the increase in absorption. Analyzing only one component, provides not necessarily the complete picture. To understand the resistance reaction on the tissue level, it might be worth to consider absorption, reflection and transmission.

Although it is not clear how far the reflected light had penetrated the leaf tissue, reflection measurements are successfully used to characterize CLS resistance and are expected to be integrated in plant phenotyping systems (Arens *et al*. 2016; Leucker *et al*. 2017). Whether the additional costs of transmission measurements are worthy is still questionable and dependent on the demand. Because the light measured by transmission passed through the whole tissue, the information is summed up over all cell layers. On the one hand, the content may be weakened due to not affected areas, like in the barley-powdery mildew interaction. Since *Blumeria graminis* f.sp. *hordei* growths epiphytically and forms haustoria only in the epidermal cells, detection was worse

using transmittance data (Thomas *et al.* 2017). On the other hand, small changes in cell metabolism or tissue structure may be more apparent due to the accumulation through all cell layers. It is more likely that minor alterations in pigment composition or cell wall applications and other defense reaction in early disease stages or in the periphery of symptom may be captured. Further research is needed to see whether the leaf transmission is useful for specific topics on plant health, for example for early disease detection, a more precise determination of the diseased leaf area or the characterization of metabolic processes during pathogen attack.

5 CONCLUSIONS

The disease severity on the sugar beet breeding lines could by visually assessed and based on the quantitative differences an estimation of the resistance to *C. beticola* was possible. No genotype was able to prevent infection completely; instead disease parameters like number and size of lesions or spore production were reduced quantitatively. Using the hyperspectral microscope, a detailed symptom analysis was possible. The differentiation of disease phenotypes based on lesion composition was improved by analyzing spectral signatures. The presented methods allowed a differentiation of CLS development depending on the host genotype and the characterization of even subtle variations in resistance. For example, differences based on the resistance source (Bv1+Q/Bv8 and Bv4_r/Bv9) or the presence of two QTL (Bv1+Q and Bv2-Q) were detectable.

With further work, also on the transmission measurements, and if the measurement procedure and data analysis are accelerated an integration into the screening process in breeding for CLS resistance is conceivable. Due to the sensitivity and the potential for automation of spectral phenotyping, a pre-selection of breeding material before field trials or a more detailed analysis of promising candidate lines may help to enhance the speed of sugar beet breeding.

6 REFERENCES

Arens N, Backhaus A, Döll S, Fischer S, Seiffert U, Mock H-P (2016) Non-invasive presymptomatic detection of *Cercospora beticola* infection and identification of early metabolic responses in sugar beet. *Frontiers* in *Plant Science* 7:1–14.

Asher MJC, Thomas CE (1984) Components of partial resistance to *Erysiphe graminis* in spring barley. Plant Pathology 33:123–130.

Barbedo JGA, Koenigkan LV, Santos TT (2016) Identifying multiple plant diseases using digital image processing. *Biosystems Engineering* 147:104-116.

Bergsträsser S, Fanourakis D, Schmittgen S, Cendrero-Mateo MP, Jansen M, Scharr H, Rascher U (2015) HyperART: non-invasive quantification of leaf traits using hyperspectral absorption-reflectance-transmittance imaging. *Plant Methods* 11:1–17.

Blackburn GA (1998) Quantifying chlorophylls and caroteniods at leaf and canopy scales. *Remote Sensing* of *Environment* 66:273–285.

Bleiholder H, Weltzien HC (1972) Beitraege zur Epidemiologie von *Cercospora beticola* Sacc. an Zuckerruebe. *Journal of Phytopathology* 73:93–114.

Carroll MW, Glaser JA, Hellmich RL, Hunt TE, Sappington TW, Calvin D, Copenhaver K, Fridgen J (2008) Use of spectral vegetation indices derived from airborne hyperspectral imagery for detection of European corn borer infestation in Iowa corn plots. *Journal of Economic Entomology* 101:1614–1623.

Daub ME, Ehrenshaft M (2000). The photoactivated *Cercospora* toxin cercosporin: contributions to plant disease and fundamental biology. Annual Review of Phytopathology 38:461–490.

De Coninck BM, Amand O, Delauré SL, Lucas S, Hias N, Weyens G, Mathys J, De Bruyne E, Cammue BP (2012) The use of digital image analysis and real-time PCR fine-tunes bioassays for quantification of Cercospora leaf spot disease in sugar beet breeding. *Plant Pathology 61:76-84*.

Delalieux S, van Aardt J, Keulemans W, Schrevens E, Coppin P (2007) Detection of biotic stress (*Venturia inaequalis*) in apple trees using hyperspectral data: Non-parametric statistical approaches and physiological implications. *European Journal of Agronomy* 27:130–143.

Di Gaspero G, Copetti D, Coleman C, Castellarin SD, Eibach R, Kozma P, Lacombe T, Gambetta G, Zvyagin A, Cindrić P, Kovács L, Morgante M, Testolin R (2012) Selective sweep at the *Rpv3* locus during grapevine breeding for downy mildew resistance. *Theoretical and Applied Genetics* 124:277–286.

Directive 2009/128/EG of the European Parliament and of the Council of 21 October 2009 establishing a framework for Community action to achieve the sustainable use of pesticide *Official Journal of the European Union* L309:71, 24.11.2009

Duffus, JE, Ruppel EG (1993) Diseases. pp 346-427 in Cooke DA, and Scott RK, eds. The Sugarbeet Crop. Chapman and Hall, London.

Feindt F, Mendgen K, Heitefuss R (1981) Der Einfluss der Spaltoeffnungsweite und des Blattalters auf den Infektionserfolg von *Cercospora beticola* bei Zuckerrueben (*Beta vulgaris* L.) unterschiedlicher Anfaelligkeit. *Phytopathologische Zeitschrift* 101:281–297.

Feindt F, Mendgen K, Heitefuss R (1980) Feinstruktur unterschiedlicher Zellwandreaktionen im Blattparenchym anfaelliger und resistenter Rueben (*Beta vulgaris* L.) nach Infektion durch *Cercospora beticola* Sacc. *Phytopathologische Zeitschrift* 101:248–264.

Fetch TG, Steffenson BJ (1999) Rating scales for assessing infection responses of barley infected with *Cochliobolus sativus*. *Plant Diseases* 83:213–217.

Feuillet C, Leach JE, Rogers J, Schnable PS, Eversole K (2011) Crop genome sequencing: lessons and rationales. *Trends in Plant Sciences* 16: 77–88.

Fischer BM, Salakhutdinov I, Akkurt M, Eibach R, Edwards KJ, Toepfer R, Zyprian EM (2004) Quantitative trait locus analysis of fungal disease resistance factors on a molecular map of grapevine. *Theoretical and Applied Genetics* 108: 501–515.

Foster DJ, Beute MK, Wynne JC (1980) Spore production and latent period as mechanisms of resistance to *Cercospora arachidicola* in four peanut genotypes. *Peanut Science* 7:88–90.

Furbank RT, Tester M (2011) Phenomics – technologies to relieve the phenotyping bottleneck. *Trends in Plant Science* 16, 635–644.

Gamon JA, Peñuelas J, Field CB (1992) A narrow-waveband spectral index that tracks diurnal changes in photosynthetic efficiency. *Remote Sensing of Environment* 41:35–44.

Geigert J, Schmitz FR, Johnson G, Maag DD, Johnson DK (1973) Two phytoalexins from sugar beet (*Beta vulgaris*) leaves. *Tetrahedron* 29:2703-2706.

Gitelson AA, Chivkunova OB, Merzlyak MN (2009) Nondestructive estimation of anthocyanins and chlorophylls in anthocyanic leaves. *American Journal of Botany* 96:1861–188.

Gitelson AA, Merzlyak MN, Chivkunova OB (2001) Optical properties and nondestructive estimation of anthocyanin content in plant leaves. *Journal of Photochemistry and Photobiology* 74:38–45.

Gottschalk TE, Mikkelsen JD, Nielsen JE, Nielsen KK, Brunstedt J (1998) Immunolocalization and characterization of a β-1,3-glucanase from sugar beet, deduction of its primary structure and nucleotide sequence by cDNA and genomic cloning. *Plant Science* 132:153–167.

Goudet C, Milat ML, Sentenac H, Thibaud JB (2000) Beticolins, nonpeptidic, polycyclic molecules produced by the phytopathogenic fungus *Cercospora beticola*, as a new family of ion channel-forming toxins. *Molecular Plant-Microbe Interactions* 13:203–209.

Govaerts YM, Jacquemoud S, Verstraete MM, Ustin SL (1996) Three-dimensional radiation transfer modeling in a dicotyledon leaf. *Applied Optics* 35:6585–6598.

Henfling JWDM, Bostock R, Kuc J (1979) Effect of abscisic acid on rishitin and lubimin accumulation and resistance to *Phytophthora infestans* and *Cladosporium cucumerinum* in potato tuber tissue slices. *Phytopathology* 70:1074–1078.

Holtschulte B (2000) *Cercospora beticola* – worldwide distribution and incidence. pp 5-16 in: Asher MJC, Holtschulte B, Richard Molard M, Rosso F, Steinrucken G, Beckers R, eds. *Cercospora beticola* Sacc. Biology, Agronomic Influence and Control Measures in Sugar Beet, Vol. 2. Advances in Sugar Beet Research. International Institute for Beet Research, Brussels, Belgium.

Hückelhoven R, Panstruga R (2011) Cell biology of the plant-powdery mildew interaction. *Current Opinion in Plant Biology* 14:738-746.

Jacquemoud S, Ustin SL (2001) Leaf optical properties: a state of the art. pp 223-332 in: 8th International Symposium of Physical Measurements & Signatures in Remote Sensing, CNES, Aussois, France.

Jensen JR (2007) Remote Sensing of the Environment: an Earth Resource Perspective. 2nd ed. Clarke KC, ed. Prentice Hall, New York.

Johnson R, Taylor AJ (1976) Spore yield of pathogens in investigations of the race - specificity of host resistance. *Annual Review of Phytopathology* 14:97 – 119.

Karadimos DA, Karaoglanidis GS, Tzavella–Klonari K (2005) Biological activity and physical modes of action of the Qo inhibitor fungicides trifloxystrobin and pyraclostrobin against *Cercospora beticola*. *Crop Protection* 24:23–29.

Karaoglanidis GS, Ioannidis PM, Thanassoulopoulos CC (2000) Reduced sensitivity of *Cercospora beticola* isolates to sterol demethylation inhibiting fungicides. *Plant Pathology* 49:567–572.

Karnovsky MJ (1965) A formaldehyde glutaraldehyde fixative of high osmolality for use in electron microscopy. Journal of Cell Biology 27:137–138.

Kirk WW, Hanson LE, Franc GD, Stump WL, Gachango E, Clark G, Stewart, J (2012) First report of strobilurin resistance in *Cercospora beticola* in sugar beet (*Beta vulgaris*) in Michigan and Nebraska, USA. N*ew Disease Reports* 26:3.

Kolmer JA (1996) Genetics of resistance to wheat leaf rust. *Annual Review of Phytopathology* 34:435–455.

Kuska M, Wahabzada M, Leucker M, Dehne HW, Kersting K, Oerke EC, Steiner U, Mahlein AK (2015) Hyperspectral phenotyping on the microscopic scale: towards automated characterization of plant-pathogen interactions. *Plant Methods* 11:28.

Leucker M, Mahlein AK, Steiner U, Oerke EC (2016) Improvement of lesion phenotyping in *Cercospora beticola* – sugar beet interaction by hyperspectral imaging. *Phytopathology* 106:177–184.

Leucker M, Wahabzada M, Kersting K, Peter M, Beyer W, Steiner U, Mahlein A-K, Oerke E-C (2017) Hyperspectral imaging reveals the effect of sugar beet quantitative trait loci on Cercospora leaf spot resistance. *Functional Plant Biology*. 2017, 44:1–9.

Lewellen RT, Whitney ED (1976) Inheritance of resistance to race C2 of *Cercospora beticola* in sugarbeet. *Crop Science* 16, 558–561.

Mahlein AK (2016) Plant disease detection by imaging sensors – parallels and specific demands for precision agriculture and plant phenotyping. *Plant Disease* 100:241–251.

Mahlein AK, Rumpf T, Welke P, Dehne H-W, Plümer L, Steiner U, Oerke EC (2013) Development of spectral indices for detecting and identifying plant diseases. *Remote Sensing of Environment* 128:21–30.

Mahlein AK, Steiner U, Dehne HW, Oerke, EC (2010) Spectral signatures of sugar beet leaves for the detection and differentiation of diseases. *Precision* Agriculture 11:413–431.

Mahlein AK, Steiner U, Hillnhuetter C, Dehne HW, Oerke, EC (2012. Hyperspectral imaging for small-scale analysis of symptoms caused by different sugar beet diseases. *Plant Methods*. 8:3.

Malthus TJ, Madeira, AC (1993) High resolution spectroradiometry: Spectral reflectance of field bean leaves infected by *Botrytis fabae*. *Remote Sensing* of *Environment* 45:107–116.

Martin SS (1977) Accumulation of the flavonoids betagarin and betavulgarin in *Beta vulgaris* infected by the fungus *Cercospora beticola*. *Physiological Plant Pathology* 11:297–303.

Meier, U. (2001) Entwicklungsstadien mono- und dikotyler Pflanzen. Biologische Bundesanstalt fuer Landwirtschaft und Forstwirtschaft. 2:1–165.

Merzlyak MN, Gitelson AA, Chivkunova OB, Rakitin VY (1999) Non-destructive optical detection of pigment changes during leaf senescence and fruit ripening. *Physiologia Plantarum* 106:135–141.

Mutka AM, Bart RS (2015) Image-based phenotyping of plant disease symptoms. *Frontiers in Plant Science* 5:1-8.

Nielsen K, Nielsen JE, Madrid SM, Mikkelsen JD (1997) Characterization of a new antifungal chitin-binding peptide from sugar beet leaves. *Plant Physiology* 113:83–91.

Niks, RE, Kuiper HJ (1983) Histology of the relation between minor and major genes for resistance of barley to leaf rust. *Phytopathology* 73:55–59.

Oerke EC, Herzog K, Toepfer R (2016) Hyperspectral phenotyping of the reaction of grapevine genotypes to *Plasmopara viticola*. *Journal of Experimental Botany* 67:5529–5543.

Oerke EC, Mahlein AK, Steiner U (2014). Proximal sensing of plant diseases. In: Gullino ML, Bonants PJM, eds. Detection and Diagnostics of Plant Pathogens in the 21st Century. 5th ed. Dordrecht: Springer Science+Business Media Dordrecht. p. 55–68.

Oerke EC, Steiner U, Dehne HW, Lindenthal M (2006) Thermal imaging of cucumber leaves affected by downy mildew and environmental conditions. *Journal of Experimental Botany* 57:2121–2132.

Parlevliet JE (1976) The genetics of seedling resistance to leaf rust, *Puccinia hordei* Otth. in some spring barley cultivars. *Euphytica* 25:249–254.

Parlevliet JE (1979) Components of resistance that reduce the rate of epidemic development. *Annual Review of Phytopathology* 17:203–222.

Peñuelas J, Filella I (1998) Visible and near-infrared reflectance techniques for diagnosing plant physiological status. *Trends in Plant Science* 3:151–156.

Richter T, Fukshansky L. (1996) Optics of a bifacial leaf: 2. Light regime as affected by the leaf structure and the light source. *Journal of Photochemistry and Photobiology* 63:517-527.

Ricker MD, Beute MK, Campbell CL (1985) Components of resistance in peanut to *Cercospora arachidicola*. *Plant Diseases* 69:1059–1064.

Rossi V, Battilani P, Chiusa G, Giosuè S, Languasco L, Racca P (1999) Components of rate-reducing resistance to Cercospora leaf spot in sugar beet: incubation length, infection efficiency, lesion size. *Journal of Plant Pathology* 81:25–35.

Rossi V, Battilani P, Chiusa G, Giosuè S, Languasco L, Racca, P. (2000) Components of rate-reducing resistance to Cercospora leaf spot in sugar beet: conidiation length, spore yield. *Journal of Plant Pathology* 82:125–131.

Rumpf T, Mahlein AK, Steiner U, Oerke EC, Dehne HW, Plümer L (2010) Early detection and classification of plant diseases with support vector machines based on hyperspectral reflectance. *Computers and Electronics in Agriculture* 74:91–99.

Ruppel, E. G. (1972) Variation among isolates of *Cercospora beticola* from sugar beet. *Phytopathology*. 62:134-136.

Savitzky A, Golay JME (1964) Smoothing and differentiation of data by simplified least squares procedures. *Analytical Chemistry* 36:1627–1639.

Schmidt K, Heberle B, Kurrasch J, Nehls R, Stahl DJ (2004) Suppression of phenylalanine ammonia lyase expression in sugar beet by the fungal pathogen *Cercospora beticola* is mediated at the core promoter of the gene. *Plant Molecular Biology* 55:835–852.

Schmidt K, Pflugmacher M, Klages S, Mäser A, Mock A, Stahl DJ (2008) Accumulation of the hormone abscisic acid (ABA) at the infection site of the fungus *Cercospora beticola* supports the role of ABA as a repressor of plant defence in sugar beet. *Molecular Plant Pathology* 9:661–673.

Scholes JD, Farrar JF (1986) Increased rates of photosynthesis in localized regions of a barley leaf infected with brown rust. *New Phytologist* 104:601–612.

Shane WW, Teng PS (1992) Impact of Cercospora leaf spot on root weight, sugar yield, and purity of *Beta vulgaris*. *Plant Diseases* 76:812-820.

Staerkel C, Boenisch MJ, Kroeger C, Bormann J, Schaefer W, Stahl, D (2013) CbCTB2, an O-methyltransferase is essential for biosynthesis of the phytotoxin cercosporin and infection of sugar beet by *Cercospora beticola*. *BMC Plant Biol*. 13:50.

Steinkamp M, Martin SS, Hoefert LL, Ruppel EG (1979) Ultrastructure of lesions produced by *Cercospora beticola* in leaves of *Beta vulgaris*. *Physiological Plant Pathology* 15:13–26.

Thomas S, Wahabzada M, Kuska MT, Rascher U, Mahlein AK (2017) Observation of plant – pathogen interaction by simultaneous hyperspectral imaging reflection and transmission measurements. *Functional Plant Biology* 44:23-35.

Trkulja N, Ivanović Ž, Pfaf-Dolovac E, Dolovac N, Mitrović M, Toševski I, Jović, J (2012) Characterisation of benzimidazole resistance of *Cercospora beticola* in Serbia using PCR-based detection of resistance-associated mutations of the β-tubulin gene. *European Journal* of *Plant Pathology* 135:889–902.

Wahabzada M, Mahlein A-K, Bauckhage C, Steiner U, Oerke E-C, Kersting K (2015) Metro maps of plant disease dynamics-automated mining of differences using hyperspectral images. *PloS one* 10:1–20.

Wahabzada M, Mahlein A-K, Bauckhage C, Steiner U, Oerke E-C, Kersting K (2016) Plant phenotyping using probabilistic topic models: uncovering the hyperspectral language of plants. *Scientific Reports* 6:22482.

Weiland J, Koch G (2004) Sugarbeet leaf spot disease (*Cercospora beticola* Sacc.). *Mol. Plant Pathology* 5:157–166.

Weltmeier F, Mäser A, Menze A, Hennig S, Schad M, Breuer F, Schulz B, Holtschulte B, Nehls R, Stahl DJ (2011) Transcript profiles in sugar beet genotypes uncover timing and strength of defense reactions to *Cercospora beticola* infection. *Molecular Plant-Microbe Interactions* 24:758–72.

West JS, Bravo C, Oberti R, Lemaire D, Moshou D, McCartney HA (2003) The potential of optical canopy measurement for targeted control of field crop diseases. *Annual Review of Phytopathology* 41:593–614.

Wetzel T, Volkmar C, Lübke-Al Hussein M, Drews FH, Jany D, Richter L (2008) Mit dem integrierten Pflanzenschutz ins neue Jahrtausend. *Archives of Phytopathology and Plant Protection* 33:299–327.

Wolf P, Verreet J (2002) The IPM sugar beet model. *Plant Diseases* 86:336–344.

Wolf P, Verreet J (2005) Factors affecting the onset of Cercospora leaf spot epidemics in sugar beet and establishment of disease-monitoring thresholds. *Phytopathology* 95:269–74.

Yuhas R, Goetz FH, Boardman JW (1992) Discrimination among semi-arid landscape endmembers using the spectral angle mapper (SAM) algorithm. In Summaries of the Third Annual JPL Airborne Geoscience Workshop, *Jet Propulsion Laboratory Publication* 92:147–149.

7 ANNEX

The following publications are essential for the present work. Due to copyright, only the abstracts are included in the online version.

Publication 1: **Hyperspectral phenotyping on the microscopic scale: towards automated characterization of plant-pathogen interactions**

Kuska M, Wahabzada M, Leucker M, Dehne H-W, Kersting K, Oerke E-C, Steiner U, Mahlein A-K (2015) *Plant Methods* 11:28–43.

Abstract

Background: The detection and characterization of resistance reactions of crop plants against fungal pathogens are essential to select resistant genotypes. In breeding practice phenotyping of plant genotypes is realized by time consuming and expensive visual rating. In this context hyperspectral imaging (HSI) is a promising non-invasive sensor technique in order to accelerate and to automate classical phenotyping methods.

A hyperspectral microscope was established to determine spectral changes on the leaf and cellular level of barley (*Hordeum vulgare*) during resistance reactions against powdery mildew (*Blumeria graminis* f.sp. *hordei*, isolate K1). Experiments were conducted with near isogenic barley lines of cv. Ingrid, including the susceptible wild type (WT), mildew locus a 12 (*Mla*12 based resistance) and the resistant mildew locus o 3 (*mlo*3 based resistance), respectively. The reflection of inoculated and non-inoculated leaves was recorded daily with a hyperspectral linescanner in the visual (400 – 700 nm) and near infrared (700 – 1000 nm) range 3 to 14 days after inoculation.

Results: Data analysis showed no significant differences in spectral signatures between non-inoculated genotypes. Barley leaves of the near-isogenic genotypes, inoculated with *B. graminis* f.sp. hordei differed in the spectral reflectance over time, respectively. The susceptible genotypes (WT, *Mla*12) showed an increase in reflectance in the visible range according to symptom development. However, the spectral signature of the resistant *mlo*-genotype did not show significant changes over the experimental period. In addition, a recent data driven approach for automated discovery of disease specific signatures, which is based on a new representation of the data using Simplex Volume Maximization (SiVM) was applied. The automated approach - evaluated in only a fraction of time revealed results similar to the time and labor intensive manually assessed hyperspectral signatures. The new representation determined by SiVM was also used to generate intuitive and easy to interpretable summaries, e.g. fingerprints or traces of hyperspectral dynamics of the different genotypes.

Conclusion: With this HSI based and data driven phenotyping approach an evaluation of host-pathogen interactions over time and a discrimination of barley genotypes differing in susceptibility to powdery mildew is possible.

Publication 2: **Improvement of lesion phenotyping in *Cercospora beticola* – sugar beet interaction by hyperspectral imaging**

Abstract

Cercospora leaf spot (CLS) caused by *Cercospora beticola* is the most destructive leaf disease of sugar beet and may cause high losses in yield and quality. Breeding and cultivation of disease resistant varieties is an important strategy to control this economically relevant plant disease. Reliable and robust resistance parameters are required to promote breeding progress. CLS lesions on five different sugar beet genotypes incubated under controlled conditions were analyzed for phenotypic differences related to field resistance to *C. beticola*. Lesions of CLS were rated by classical quantitative and qualitative methods in combination with non-invasive hyperspectral imaging. Calculating the ratio of lesion center to lesion margin four CLS phenotypes were identified which vary in size and spatial composition. Lesions could be differentiated into subareas based on their spectral characteristics in the range 400 to 900 nm. Sugar beet genotypes with lower disease severity typically had lesions with smaller centers compared to highly susceptible genotypes. Accordingly, the number of conidia per diseased leaf area on resistant plants was lower. The assessment of lesion phenotypes by hyperspectral imaging with regard to sporulation may be an appropriate method to identify subtle differences in disease resistance. The spectral and spatial analysis of the lesions has the potential to improve the screening process in breeding for CLS resistance.

Publication 3: **Hyperspectral imaging reveals the effect of sugar beet quantitative trait loci on Cercospora leaf spot resistance**

Leucker M, Wahabzada M, Kersting K, Peter M, Beyer W, Steiner U, Mahlein A-K, Oerke E-C (2017) *Functional Plant Biology* 44:1–9.

Abstract

The quantitative resistance of sugar beet (*Beta vulgaris* L.) against Cercospora leaf spot (CLS) caused by *Cercospora beticola* (Sacc.) was characterised by hyperspectral imaging. Two closely related inbred lines, differing in two quantitative trait loci (QTL), which made a difference in disease severity of 1.1–1.7 on the standard scoring scale (1–9), were investigated under controlled conditions. The temporal and spatial development of CLS lesions on the two genotypes were monitored using a hyperspectral microscope. The lesion development on the QTL-carrying, resistant genotype was characterised by a fast and abrupt change in spectral reflectance, whereas it was slower and ultimately more severe on the genotype lacking the QTL. An efficient approach for clustering of hyperspectral signatures was adapted in order to reveal resistance characteristics automatically. The presented method allowed a fast and reliable differentiation of CLS dynamics and lesion composition providing a promising tool to improve resistance breeding by objective and precise plant phenotyping.